Linker dependence of $^1O_2$ generation by G4-binding tetra-imidazolium porphyrins

Çetin Çelik[a], Naoko Kakusho[b], Tianyu Xu[a], Sung Sik Lee[c], Naoko Yoshizawa-Sugata,[d]* Hisao Masai[b]* and Yoko Yamakoshi [a]*

[a]*Department of Chemistry and Applied Biosciences, ETH Zürich, Vladimir-Prelog-Weg 3, CH-8093 Zürich, Switzerland.* [b]*Department of Basic Medical Sciences, Tokyo Metropolitan Institute of Medical Science, 2-1-6 Kamikitazawa, Setagaya, Tokyo 156-8506, Japan.* [c]*ScopeM, ETH Zürich, Otto-Stern-Weg 3, CH-8093 Zürich, Switzerland.* [d]*Research Center for Genome & Medical Sciences, Tokyo Metropolitan Institute of Medical Science, 2-1-6 Kamikitazawa, Setagaya, Tokyo 156-8506, Japan.*

–Supporting information–

1.Syntheses of compounds 1, 2 and 3

General. NMR spectra were recorded at room temperature on Bruker Avance III HD 400 MHz and Bruker Neo 400 MHz (Bruker BioSpin GmbH, Ettlingen, Germany) using solvent peaks as standards (*e.g.* $CDCl_3$ (7.26 ppm), DMSO-d_6 (2.50 ppm) or D_2O (4.79 ppm) for ^{1}H-NMR and $CDCl_3$ (77.16 ppm) or DMSO-d_6 (39.52 ppm) for ^{13}C-NMR. HRMS spectra were recorded on Bruker Daltonics maXis ESI-QTOF spectrometer (Bruker Daltonics GmbH, Bremen, Germany). FT-IR spectra were recorded on a JASCO 4100 FT-IR Spectrometer equipped with an ATR Pro One (JASCO, Inc., Tokyo, Japan). Reverse phase analytical HPLC analyses were performed using Shiseido Capcell Pak C18 4.6ID×250mm (Osaka Soda Co., Ltd., Osaka, Japan). Reverse phase preparative HPLC were conducted using a YMC-Pack ODS-A 250 x 20 I.D. column (YMC Co. Ltd., Kyoto, Japan). Column chromatography was performed on SiliaFlash P60, 230-400 mesh (Silicycle, Quebec, Canada) or SiO_2 high-purity grade cat. #9385, 230-400 mesh (Sigma-Aldrich, St. Louis, MO, USA). TLC were performed on Silica gel 60 F254 plates (Merck KGaA, Darmstadt, Germany). Four-hydroxybenzaldehyde, 1,2-dibromoethane, 1,3-dibromopropane, 1,4-dibromobutane, 1-methyl imidazole, MeOH, NaOH, trifluoroacetic acid (TFA) were purchased from Sigma-Aldrich (St. Louis, Missouri, USA). $CDCl_3$, DMSO-d_6, D_2O, BF_3OEt_2, Four,5-dichloro-3,6-dioxocyclohexa-1,4-diene-1,2-dicarbonitrile (DDQ) was purchased from Apollo Scientific (Manchester, UK). Dowex® 1X8-200 Cl^- were purchased from abcr GmbH (Karlsruhe, Germany). HCl 37% was purchased from VWR International (Radnor, PA, USA). All aqueous solutions were prepared by using MilliQ water.

All chemicals were used as received except for pyrrole, which was distilled prior to use. All dry solvents were purchased from Acros and were used as received. Ethyl Acetate (EtOAc), hexane, methanol, and dichloromethane were purchased from Thommen Furler AG (Rüti b. Büren, Switzerland). HPLC-grade toluene, MeCN, CH_2Cl_2, and $CHCl_3$ were purchased from Sigma-Aldrich.

Scheme S1. Synthesis of compounds **1, 2** and **3**.

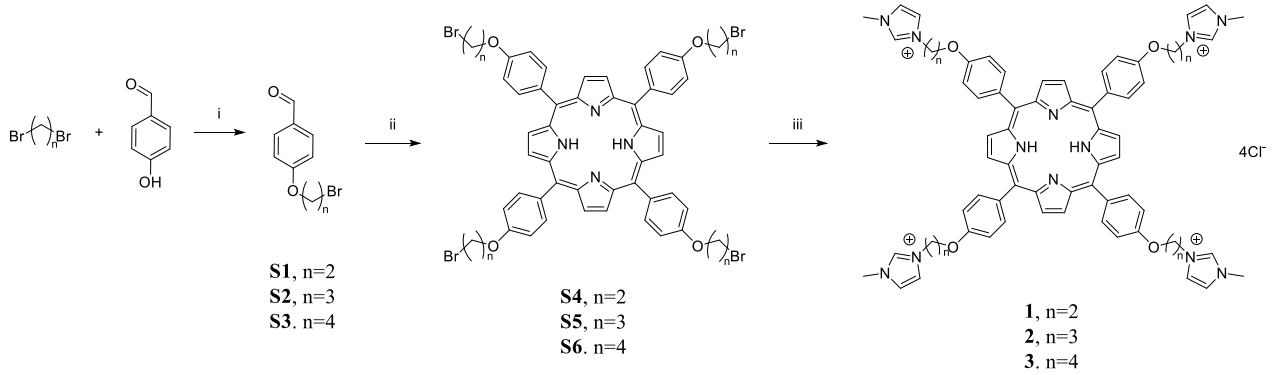

S1, n=2
S2, n=3
S3. n=4

S4, n=2
S5, n=3
S6. n=4

1, n=2
2, n=3
3. n=4

Reagents and conditions: i) K_2CO_3, DMF, rt, 16 h; ii) BF_3OEt_2, pyrrole, CH_2Cl_2, rt, 1 h, then DDQ, 1 h; iii) 1-methylimidazole, 80 °C, 14 h, then Dowex 1x8 (200) Cl^- form.

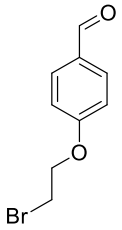

Compound S1. To a solution of the 4-hydroxybenzaldehyde (4 g, 33 mmol) in DMF (50 mL), 1,2-dibromoethane (30 mL, 340 mmol) and K_2CO_3 (69 mmol, 9.6 g) was added and stirred overnight at room temperature under N_2. To the reaction mixture, water (100 mL) was added and was extracted using Et_2O. Organic layer was washed with water two times and then with brine. The resulting organic layer was dried over Na_2SO_4 and concentrated in vacuo. The residue was recrystallized from hexane to provide **S1** as colourless crystals (5.9 g, 26 mmol, y = 75%); ^{1}H-NMR (400 MHz, $CDCl_3$): δ_H 3.68 (t, J = 6.4 Hz, 2H, CH_2-C**H₂**-Br), 4.39 (t, J = 6.3 Hz, 2H, O-C**H₂**), 7.02 (dt, J = 8.7 Hz, 2H, Ar**H** meta to CHO), 7.87 (dt, J = 8.9 Hz, 2H, Ar**H** ortho to CHO), 9.90 (s, 1H, C**H**O); HRMS (ESI$^+$) m/z calcd. for $C_9H_{10}BrO_2^+$: 228.9859, found: 228.9854 ([M+H]$^+$).

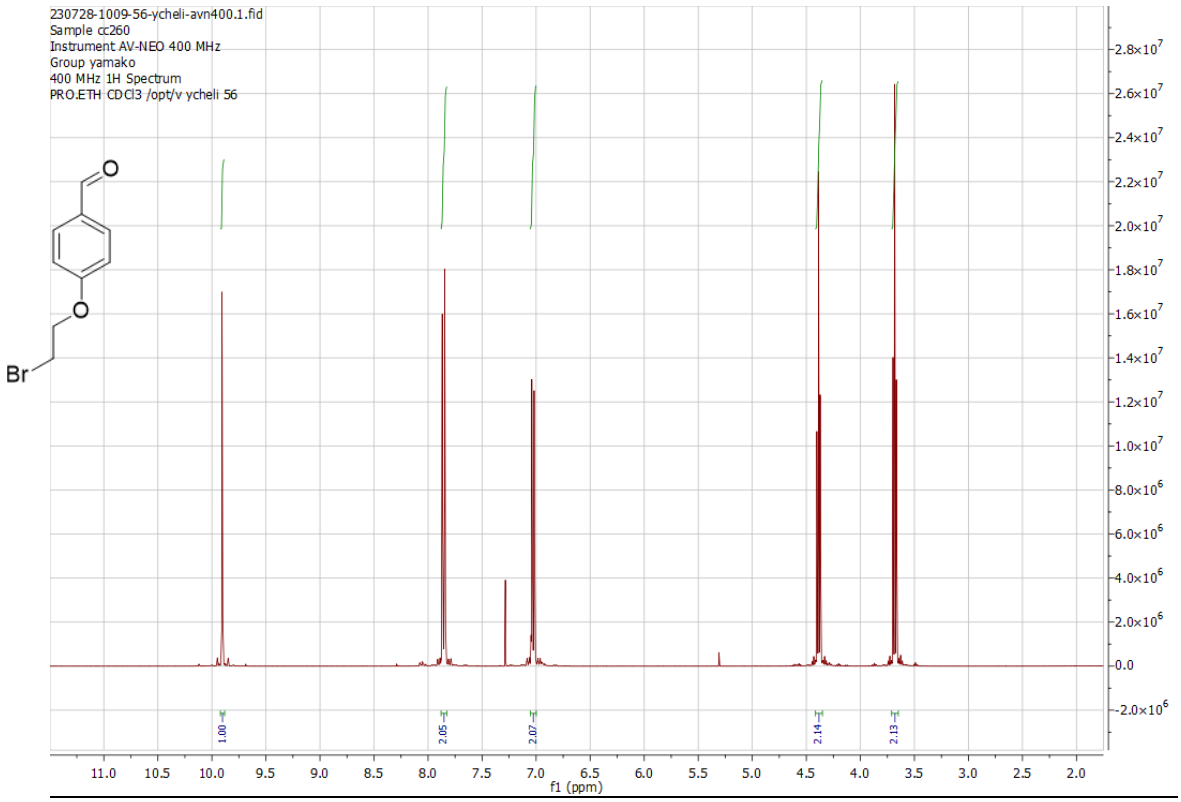

Fig. S1. ^{1}H-NMR spectrum of **S1** (400 MHz, $CDCl_3$).

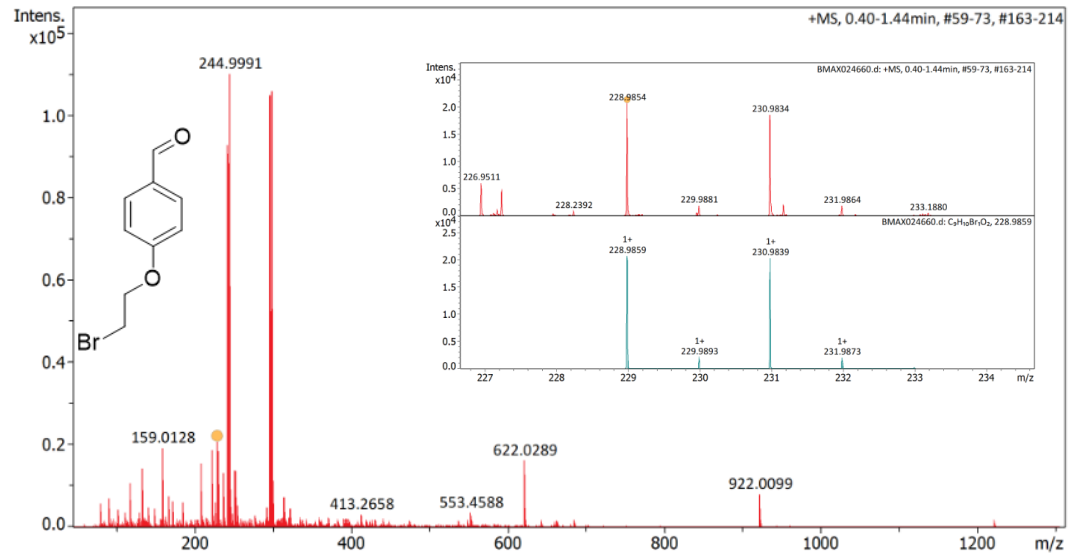

Fig. S2. Measured (inset top) and simulated (inset bottom) HR-ESI-MS spectra of **S1**.

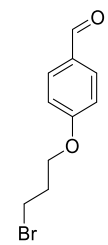

Compound S2. To a solution of the 4-hydroxybenzaldehyde (5 g, 41 mmol) in DMF (50 mL), 1,3-dibromopropane (20 mL, 204 mmol) was added and stirred overnight at room temperature under N_2. To the reaction mixture, water (100 mL) was added and was extracted using Et_2O. Organic layer was washed with water two times and then with brine. The resulting organic layer was dried over Na_2SO_4 and concentrated in vacuo. The residue was recrystallized from hexane to provide **S2** as colourless crystals (8.2 g, 33 mmol, y = 82%); ^{1}H-NMR (400 MHz, $CDCl_3$): δ_H

2.34 (quintet, J = 6.3 Hz, 2H, O-CH$_2$-**CH$_2$**-CH$_2$-Br), 3.60 (t, J = 6.4 Hz, 2H, CH$_2$-C**H$_2$**-Br), 4.19 (t, J = 5.8 Hz, 2H, O-C**H$_2$**), 7.00 (dt, J = 8.74, 2.84 Hz, 2H, Ar**H**, meta to CHO), 7.82 (dt, J = 8.9, 2.6 Hz, 2H, Ar**H** ortho to CHO), 9.87 (s, 1H, C**H**O); HRMS (ESI$^+$) *m/z* calcd. for $C_{10}H_{12}BrO_2^+$: 243.0015, found: 243.0013 ([M+H]$^+$).

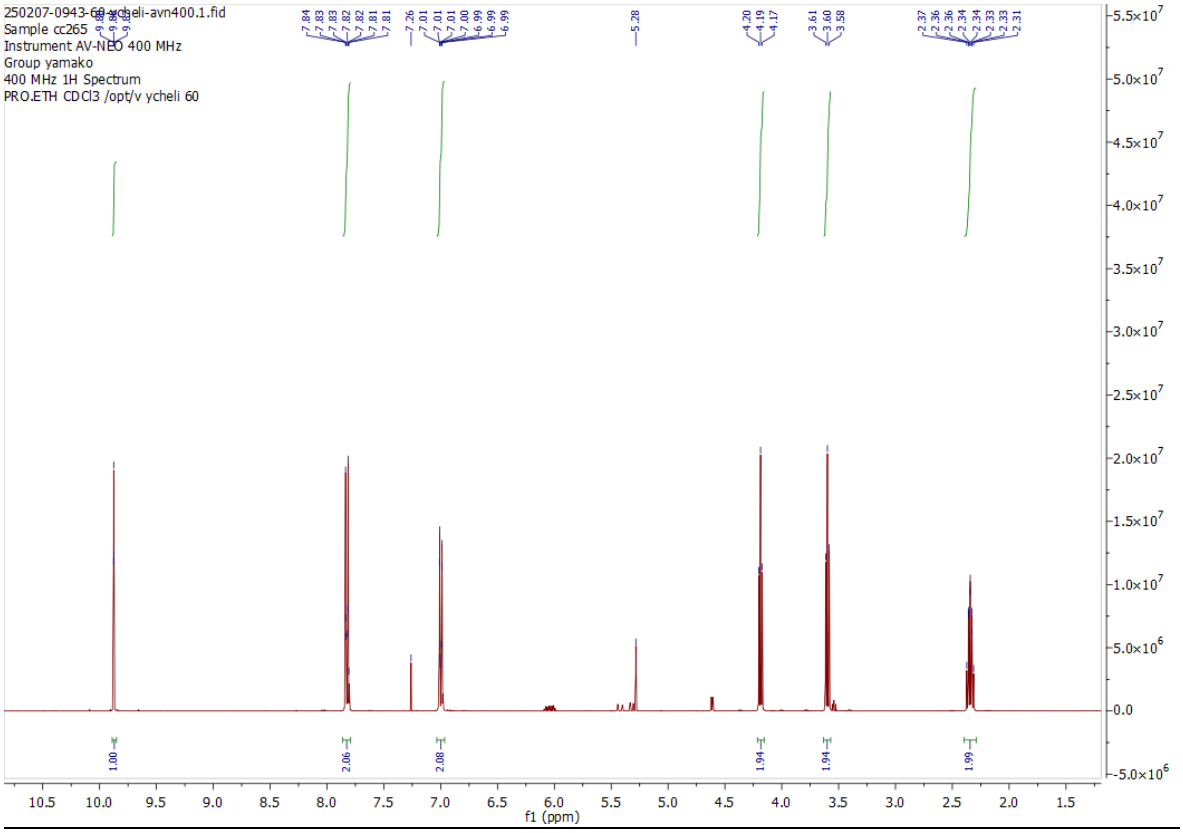

Fig. S3. ^{1}H-NMR spectrum of **S2** (400 MHz, $CDCl_3$).

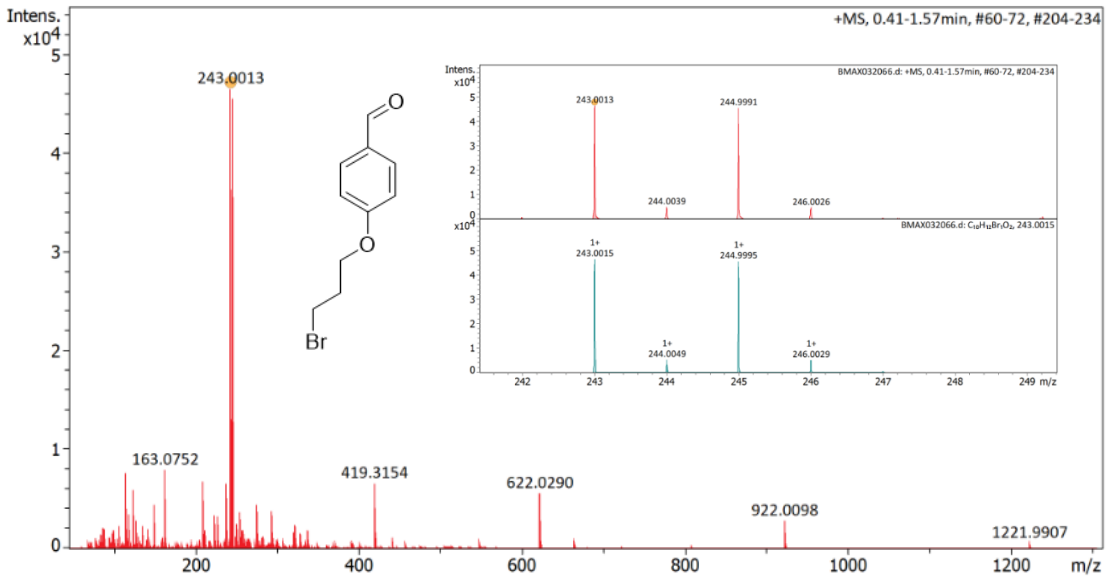

Fig. S4. Measured (inset top) and simulated (inset bottom) HR-ESI-MS spectra of **S2**.

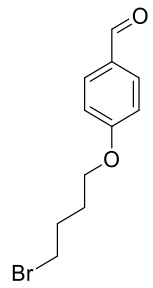

Compound S3. To a solution of the 4-hydroxybenzaldehyde (5 g, 41 mmol) in DMF (50 mL), 1,4-dibromobutane (24 mL, 200 mmol) was added and stirred overnight at room temperature under N_2. To the reaction mixture, water (100 mL) was added and was extracted using Et_2O. Organic layer was washed with water two times and then with brine. The resulting organic layer was dried over Na_2SO_4 and concentrated in vacuo. The residue was recrystallized from hexane to provide **S3** as colourless crystals (10.2 g, 39 mmol, y = 96%); ^{1}H-NMR (400 MHz, $CDCl_3$): δ_H 2.02 (m, 2H, CH_2-**CH_2**-CH_2-Br) 2.05 (m, 2H, O-CH_2-**CH_2**-CH_2), 3.48 (t, J = 6.4 Hz, 2H, CH2-C**H2**-Br), 4.07 (t, J = 5.8 Hz, 2H, O-C**H_2**), 6.97 (d, J = 8.7 Hz, 2H, Ar**H**, meta to CHO), 7.82 (J = 8.7 Hz, 2H, Ar**H** ortho to CHO), 9.87 (s, 1H, C**H**O).

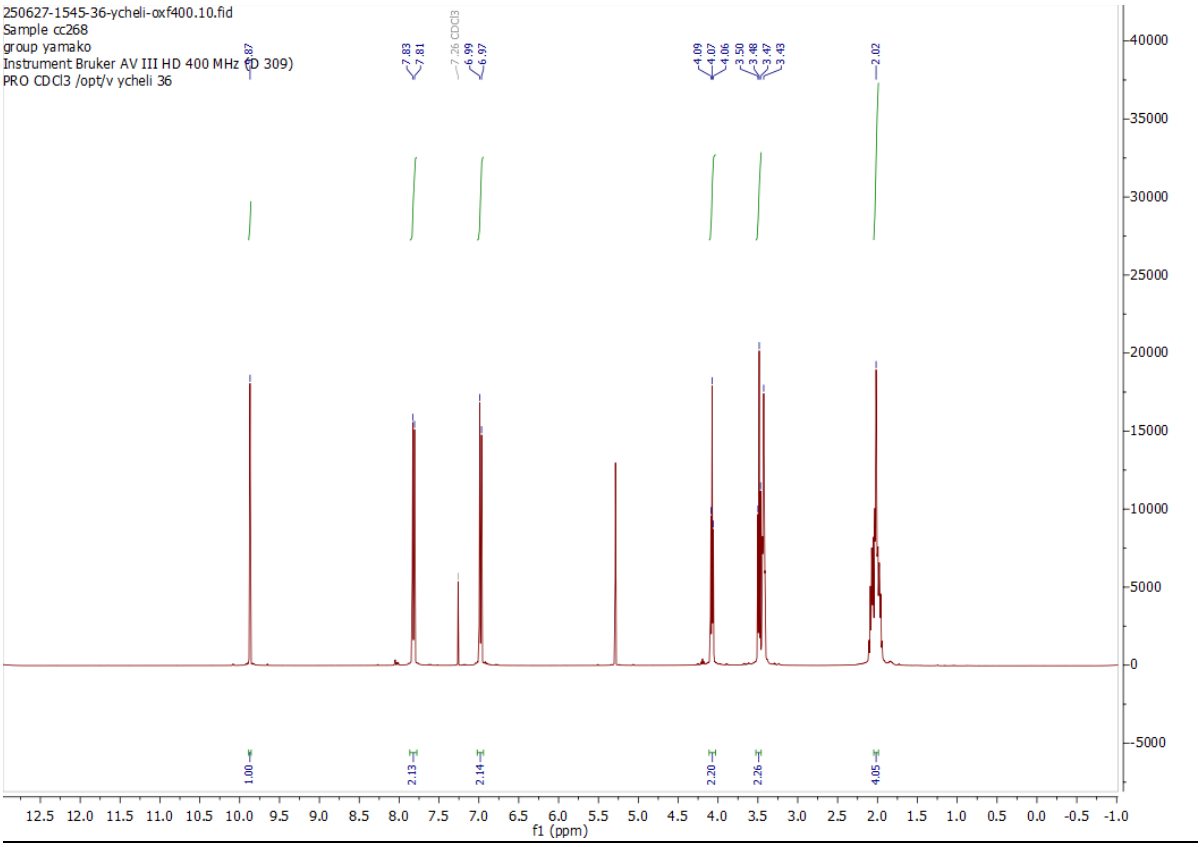

Fig. S5. ^{1}H-NMR spectrum of **S3** (400 MHz, $CDCl_3$).

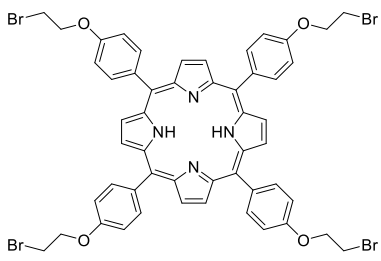

Compound S4. To a solution of **S1** (1.00 g, 4.36 mmol) in CH_2Cl_2 (500 mL), pyrrole (0.30 mL, 4.36 mmol) was added and N_2 was bubbled for 10 min. Subsequently, BF_3OEt_2 (0.05 mL, 0.41 mmol) was added and the reaction mixture was stirred at room temperature for 1 h under N_2 atmosphere. Then DDQ (0.74 g, 3.27 mmol) was added and the mixture was stirred further 1 h. The reaction mixture was directly added to a column and eluted by

toluene:acetone 30:1 to provide **S4** as purple solids with **S1** as impurity (0.39 g, 0.35 mmol, crude y = 32%); HRMS (ESI$^+$) *m/z* calcd. for $C_{52}H_{43}Br_4N_4O_4^+$: 1103.0012, found: 1103.0013 ([M+H]$^+$).

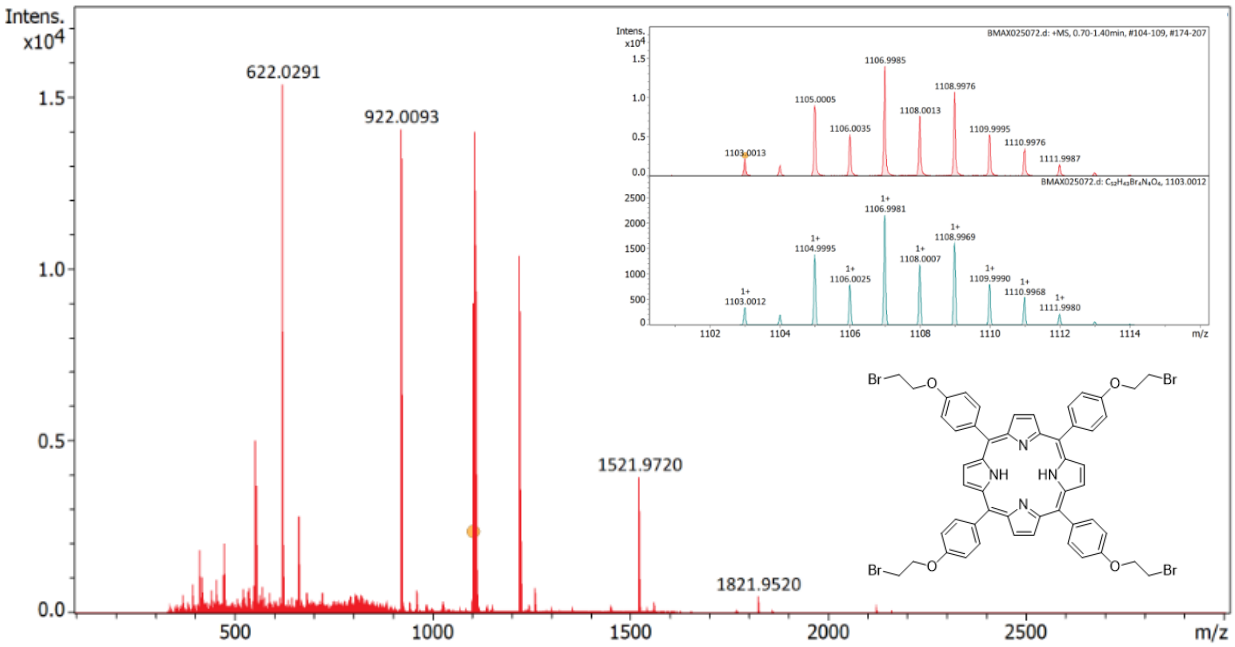

Fig. S6. Measured (inset top) and simulated (inset bottom) HR-ESI-MS spectra of **S4**.

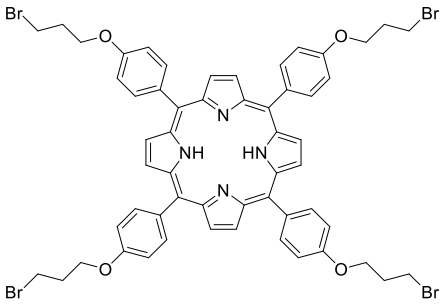

Compound S5. To a solution of **S2** (2.01 g, 8.22 mmol) in CH_2Cl_2 (500 mL), pyrrole (0.57 mL, 8.22 mmol) was added and N_2 was bubbled for 10 min. Subsequently, BF_3OEt_2 (0.10 mL, 0.81 mmol) was added and the reaction mixture was stirred at room temperature for 1 h under N_2 atmosphere. Then DDQ (1.40 g, 6.42 mmol) was added and the mixture was stirred further 1 h. The reaction mixture was directly added to a column and eluted by toluene:acetone 30:1 to provide **S5** as purple solids (0.39 g, 0.35 mmol, y = 17%); ^{1}H-NMR (400 MHz, $CDCl_3$) δ_H –2.75 (2H, br s, pyrrolic N**H**), 2.52 (quintet, *J* = 6.1 Hz, 8H, O-CH_2-**CH_2**-CH_2-Br), 3.79 (t, *J* = 6.4 Hz, 8H, CH_2-**CH_2**-Br), 4.41 (t, *J* = 5.7 Hz, 8H, O-**CH_2**), 7.29 (dt, *J* = 8.7, 2.2 Hz, 8H, Ar**H**, meta to porphyrin), 8.11 (dt, *J* = 8.7, 2.0 Hz, 8H, Ar**H** *ortho* to porphyrin), 8.86 (8H, s, β-pyrrole-**H**); HRMS (MALDI+) *m/z* calcd. for $C_{56}H_{50}Br_4N_4O_4^+$: 1158.0560, , found: 1158.0565 (M^+).

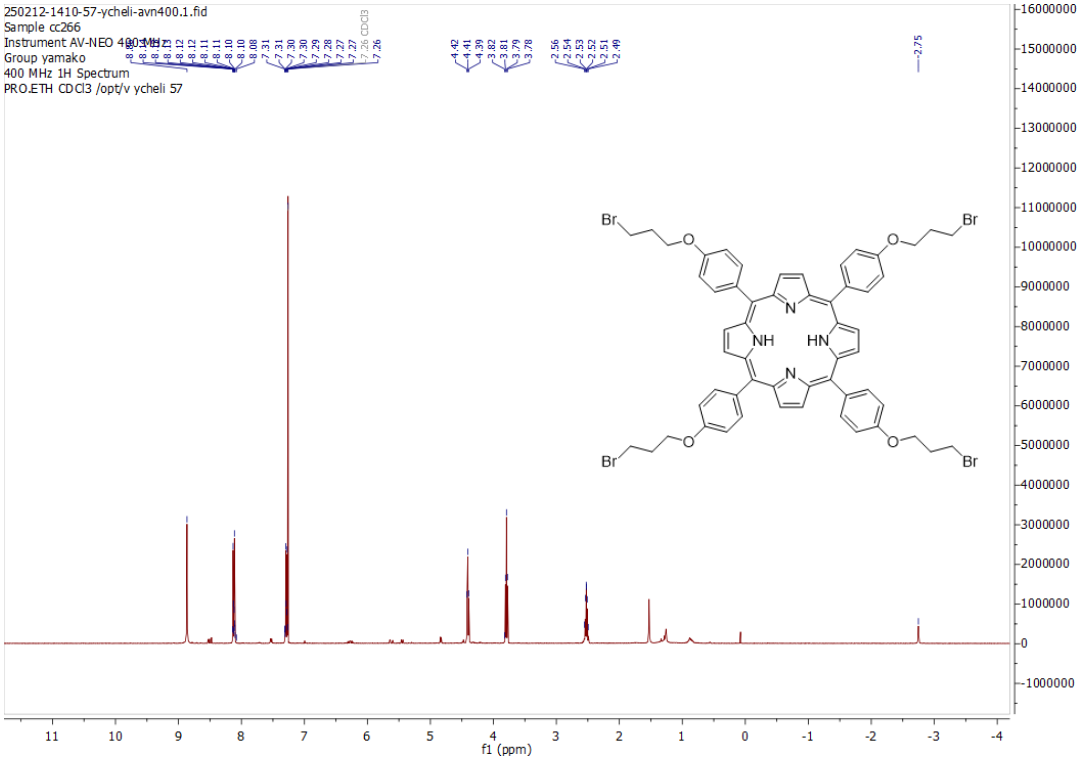

Fig. S7. ^{1}H-NMR spectrum of **S5** (400 MHz, $CDCl_3$).

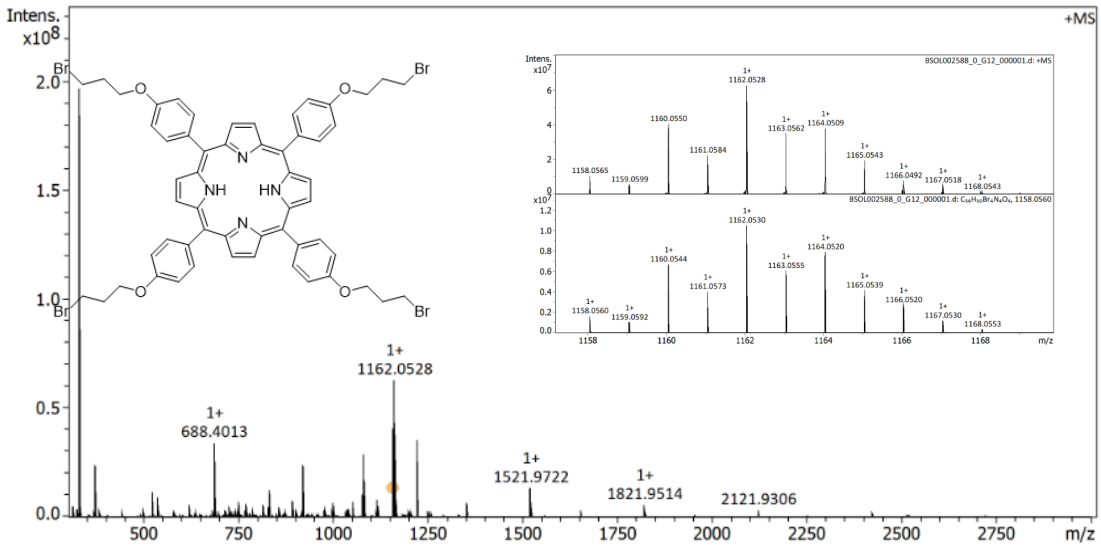

Fig. S8. Measured (inset top) and simulated (inset bottom) HR-MALDI-MS spectra of **S5**.

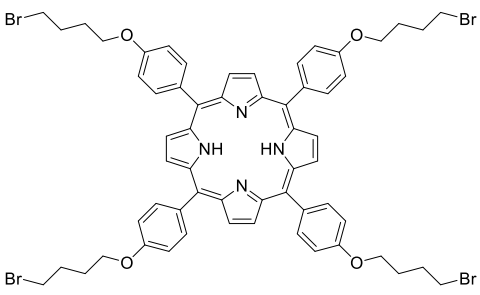

Compound S6. To a solution of **S3** (1.99 g, 7.78 mmol) in CH_2Cl_2 (500 mL), pyrrole (0.54 mL, 7.78 mmol) was added and N_2 was bubbled for 10 min. Subsequently, BF_3OEt_2 (0.09 mL, 0.78 mmol) was added and the reaction mixture was stirred at room temperature for 1 h under N_2 atmosphere. Then DDQ (1.32 g, 5.83 mmol) was added and the mixture was stirred further 1 h. The reaction mixture was directly added to a column and eluted by toluene:acetone 30:1 to provide **S6** as

purple solids with **S3** as impurity (0.76 g, 0.62 mmol, crude y = 32%); HRMS (MALDI$^+$) *m/z* calcd. for $C_{60}H_{58}Br_4N_4O_4^+$: 1214.1186, found: 1214.1195 (M^+).

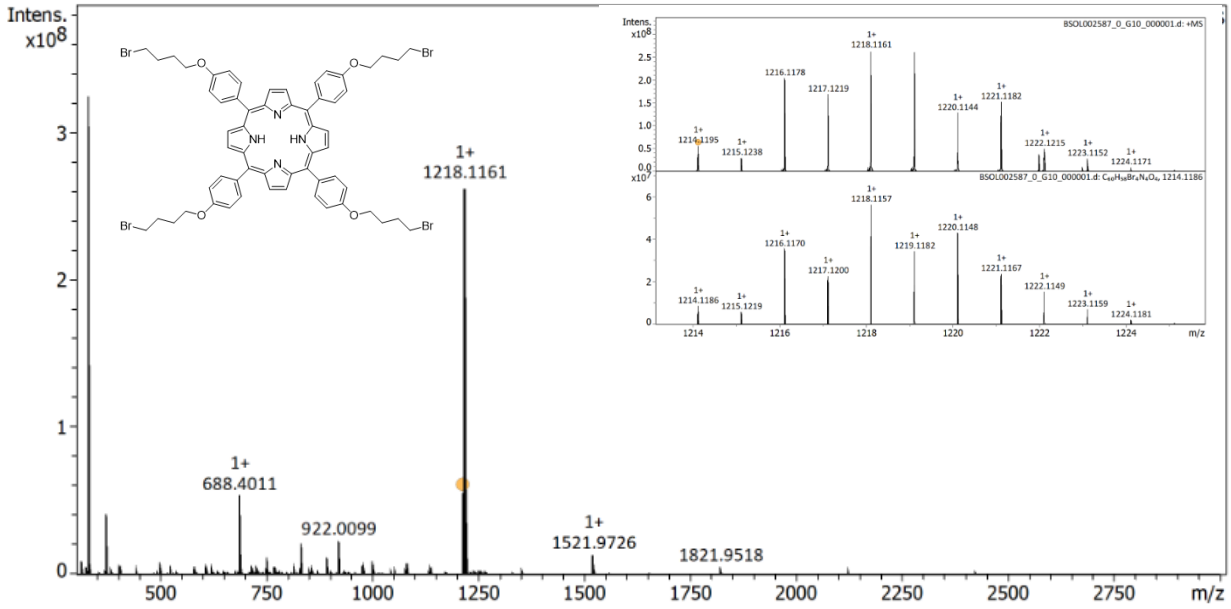

Fig. S9. Measured (inset top) and simulated (inset bottom) HR-MALDI-MS spectra of **S6**.

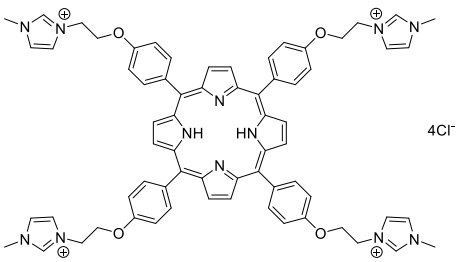

Compound 1. To a solution of **S4** (70 mg, 0.10 mmol) in 1-methylimidazole (5 mL), N_2 was bubbled for 10 min. The reaction mixture was stirred at 80 °C for 14 h, and then cooled to room temperature. The reaction mixture was concentrated *in vacuo* and the residue was dissolved in MeOH and precipitated by Et_2O. The solvent was decanted off and the precipitate was washed with Et_2O multiple times. The crude mixture was purified by a reverse phase HPLC (column: column: YMC-Pack ODS-A F20 mm x 250 mm; solvents MeCN-H_2O (10% to 40% MeCN gradient over 30 min) containing 0.1% TFA)) to provide compound **1** in a TFA salt form. The product was stirred overnight with DOWEX 1x8-200 resin (5 g) in water (10 mL) to have chloride as a counter anion. The mixture was filtered on sintered glass and the filtrate was concentrated *in vacuo*, lyophilized, and analyzed by HPLC to confirm the purity, to provide compound **1** as green fluffy solids (60 mg, 0.047 mmol, y = 75%); mp > 300 °C; FT-IR (ATR) υ_{max} (cm^{-1}): 3396, 3151, 3099, 1671, 1604, 1575, 1503, 1467, 1417, 1351, 1286, 1293, 1167, 1107, 1054, 965, 911, 827, 797, 737, 716, 656, 620; ^{1}H-NMR (400 MHz, DMSO-d_6) δ_H –-2.92 (br s, 2H, inner N-**H**), 3.99 (s, 12H, N-C**H**$_3$), 4.68 (t, J = 4.3 Hz, 8H, O-CH$_2$-C**H**$_2$-N), 4.81 (t, J = 4.3 Hz, 8H, Ar-O-C**H**$_2$-CH$_2$), 7.42 (d, J = 8.6 Hz, 8H, Ph-**H**, *meta* to porphyrin), 7.86 (t, J = 1.7 Hz, 4H, imidazole 4'C-**H**), 8.01 (t, J = 1.8 Hz, 4H, imidazole 5'C-**H**), 8.15 (d, J = 8.6, 8H, Ar-**H**, *ortho* to porphyrin), 8.83 (s, 8H, β-pyrrole-**H**), 9.41 (s, 4H, imidazole 2'C-**H**) ^{13}C-NMR (100 MHz, DMSO-d_6) δ 35.90 (imidazole, N-**C**H$_3$). 48.70 (O-**C**H$_2$-CH$_2$-N), 66.05 (O-CH$_2$-**C**H$_2$-N), 113.20 (Ar-**C**, *meta* to porphyrin), 123.01 (imidazole 5'**C**), 123.67 (imidazole

4'**C**), 131.25 (broad, β-pyrrole **C**), 134.19 (Ar**C**, *ipso* to porphyrin), 135.35 (Ar**C**, *ortho* to porphyrin), 137.28 (imidazole 2'**C**), 157.68 (Ar**C**, *para* to porphyrin); HRMS (ESI$^+$) *m/z* calcd. for $C_{68}H_{66}N_{12}O_4^{4+}$: 278.6327, found: 278.6330 (M^{4+}).

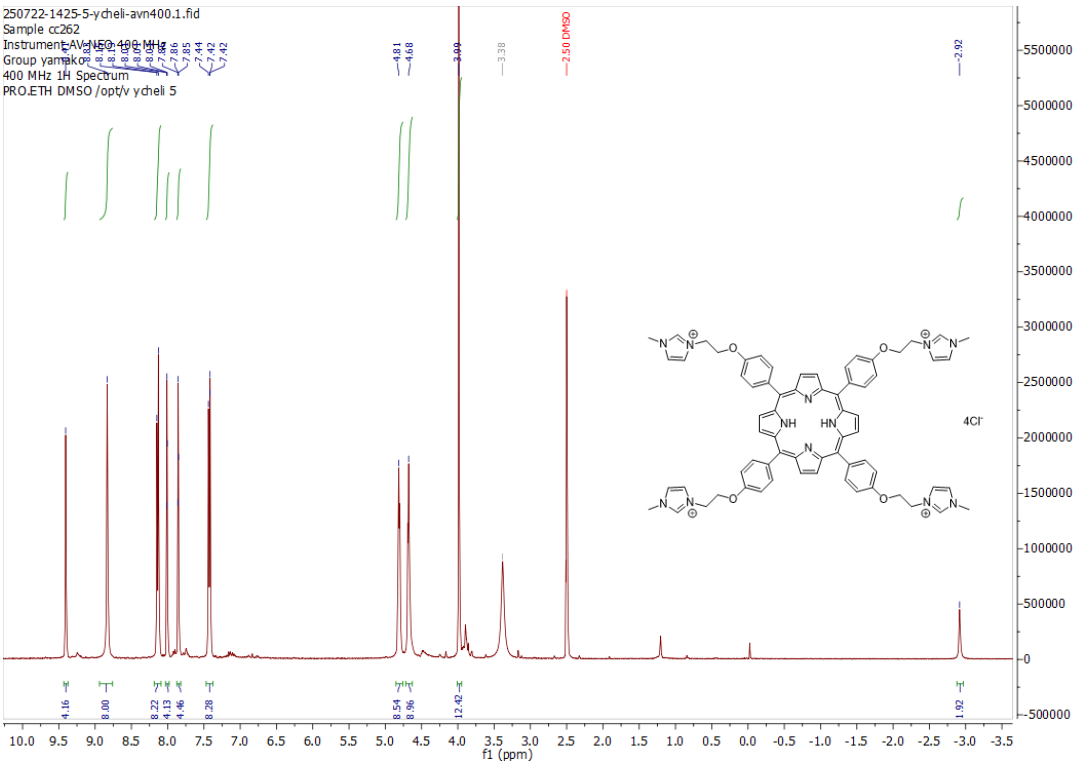

Fig. S10. ^{1}H-NMR spectrum of **1** (400 MHz, DMSO-*d*$_6$).

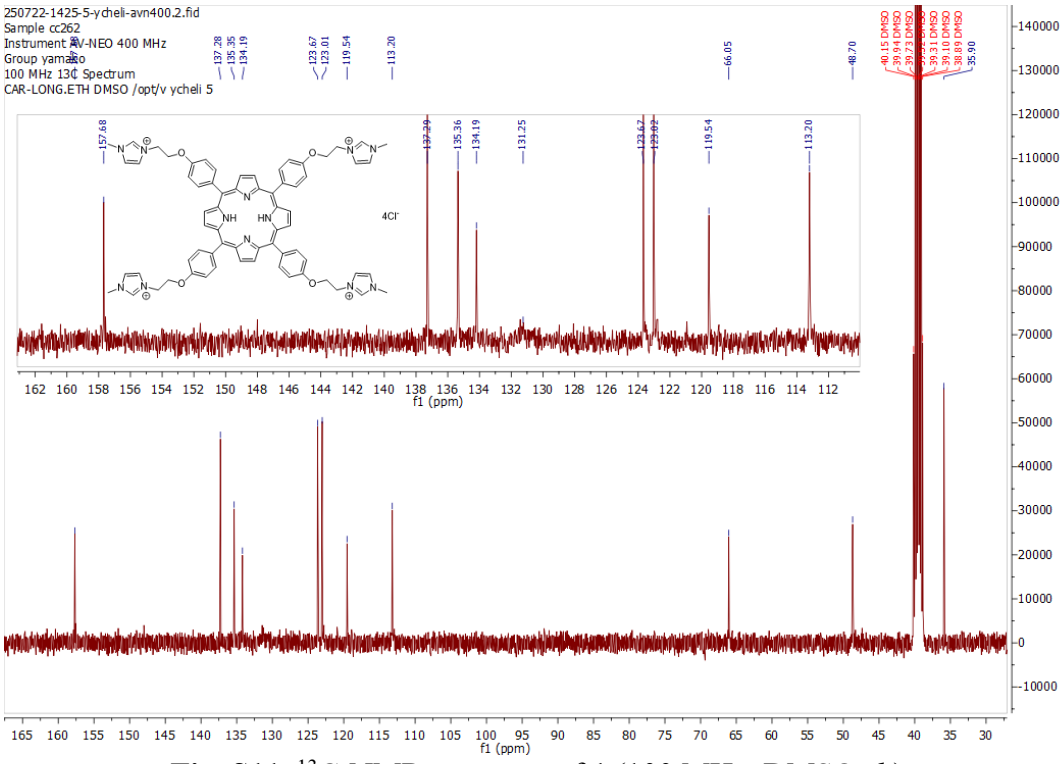

Fig. S11. ^{13}C-NMR spectrum of **1** (100 MHz, DMSO-*d*$_6$).

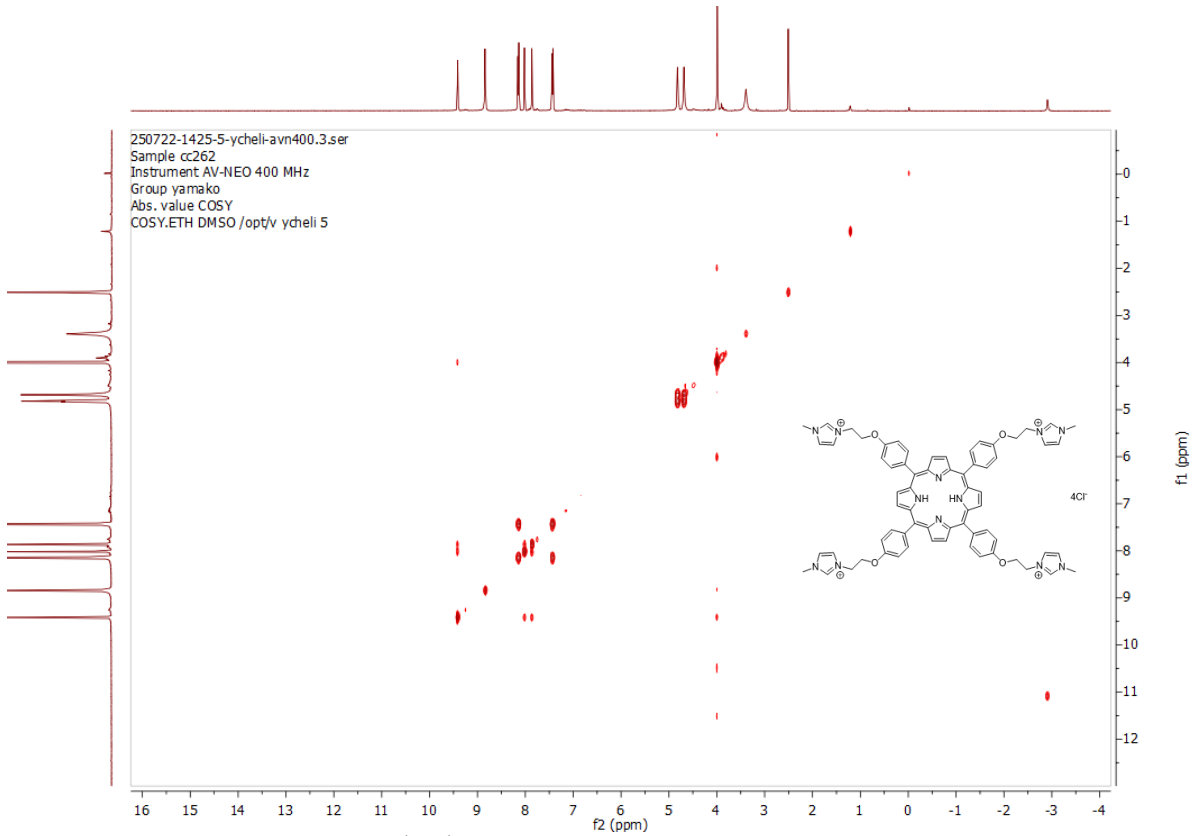

Fig. S12. $^{1}H/^{1}H$ COSY spectrum of **1** (DMSO-d_6).

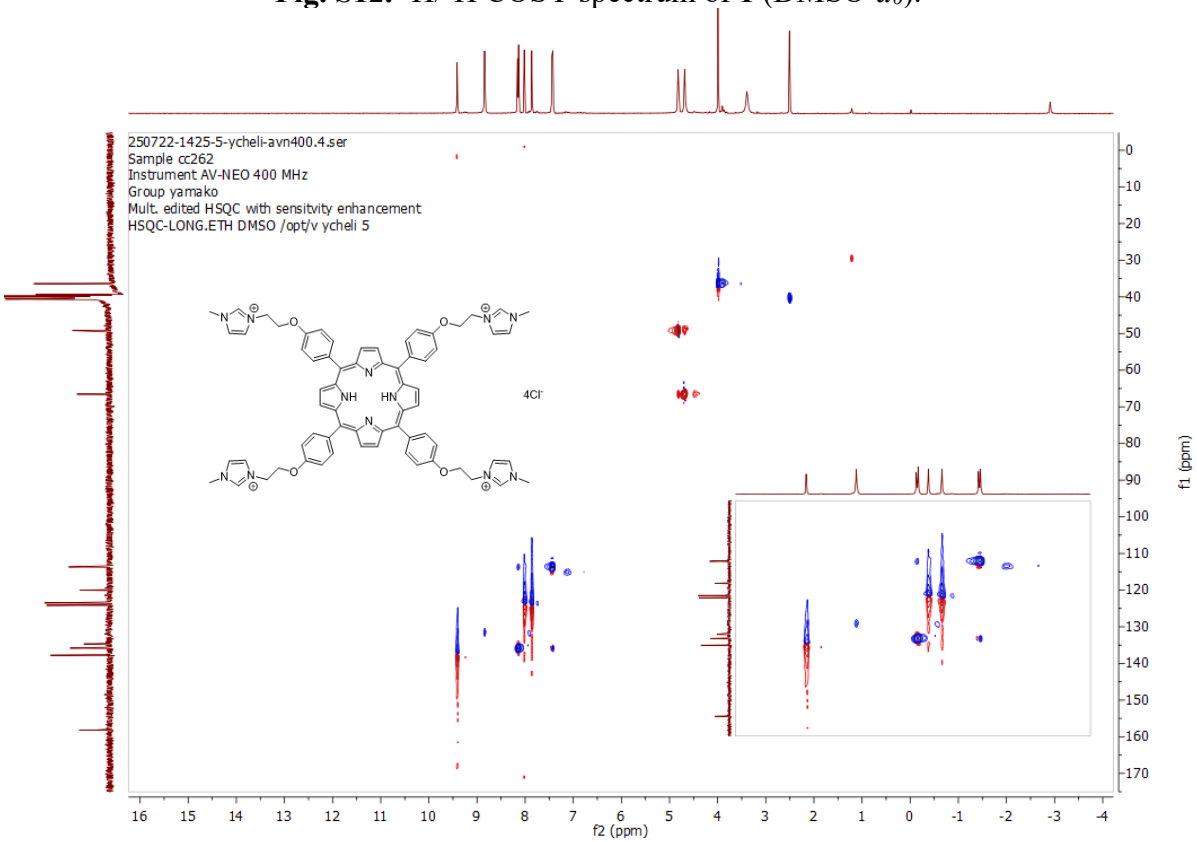

Fig. S13. HSQC-NMR spectrum of **1** (DMSO-d_6).

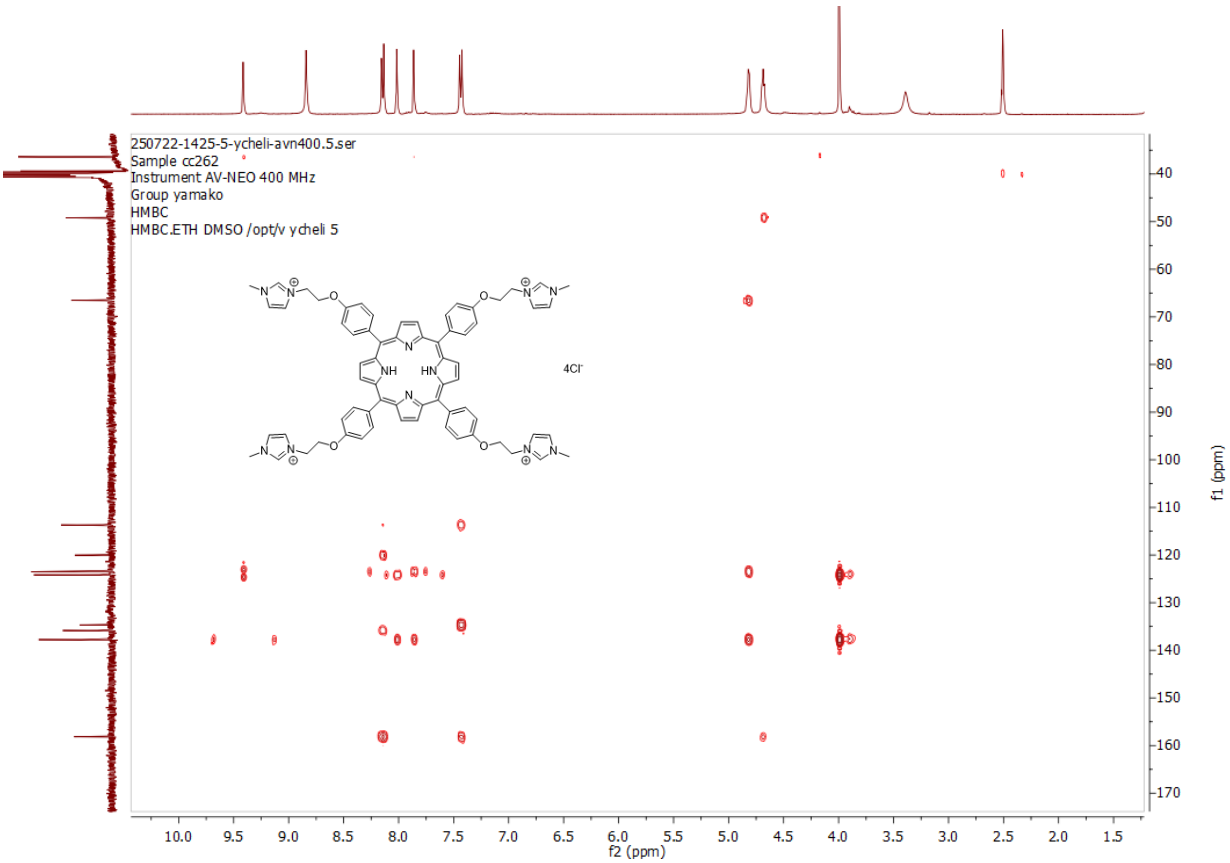

Fig. S14. HMBC-NMR spectrum of **1** (DMSO-d_6).

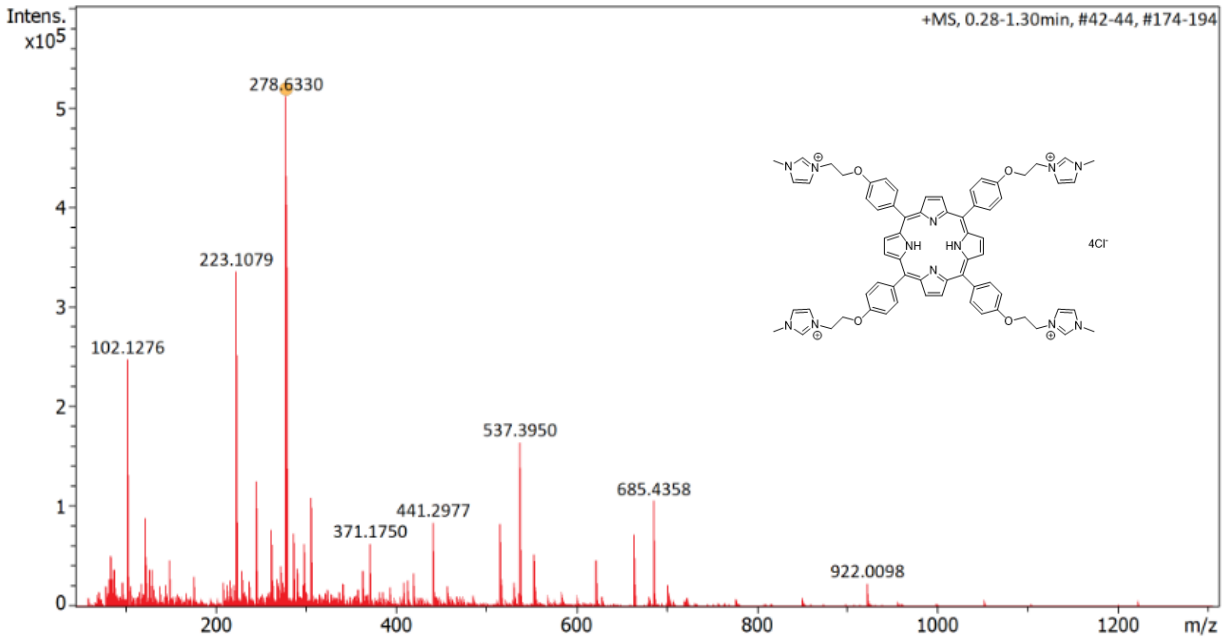

Fig. S15. Measured (inset top) and simulated (inset bottom) HR-ESI-MS spectra of **1**.

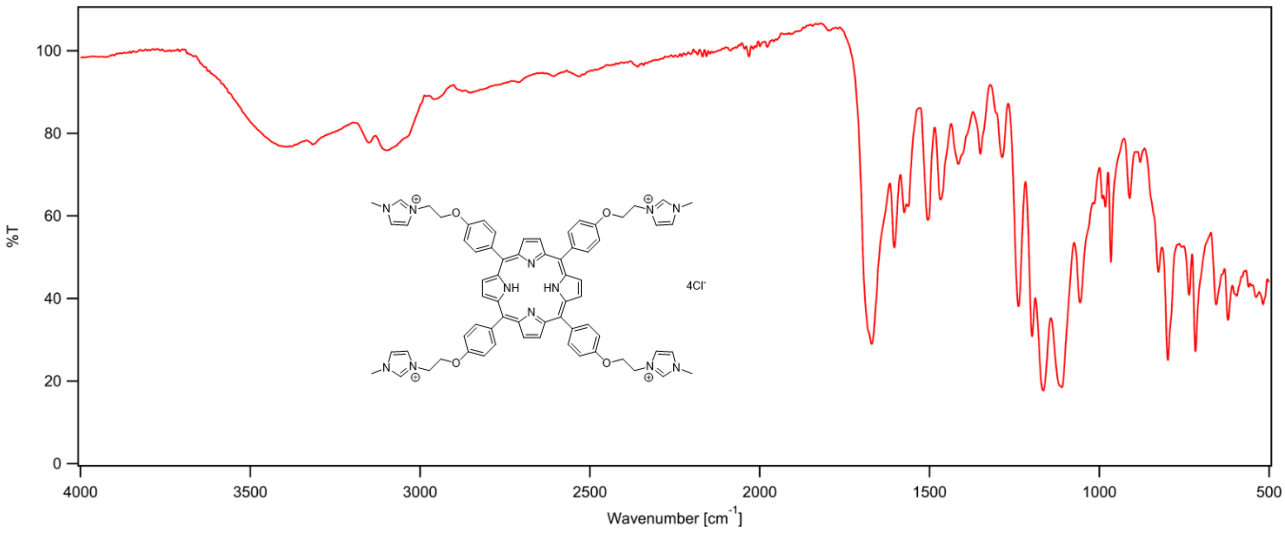

Fig. S16. FT-IR ATR spectrum of **1**.

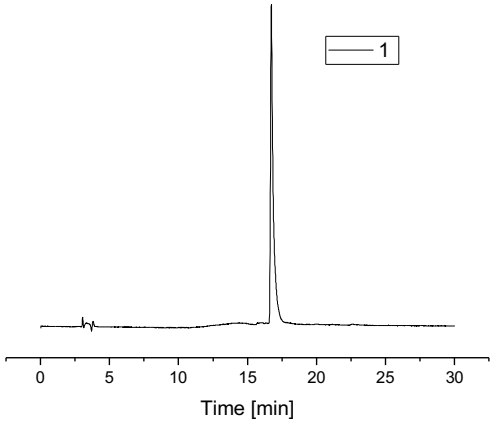

Fig. S17. RP-HPLC chromatogram of **1** (Column: Shiseido Capcell Pack C18 (4.6 mm x 250 mm); solvents: H_2O - MeCN (90:10 for 3 min, gradient to 10:90 over 22 min, then 10:90 for 5 min); flow rate: 1 mL•min^{-1}; detection: 220 nm.)

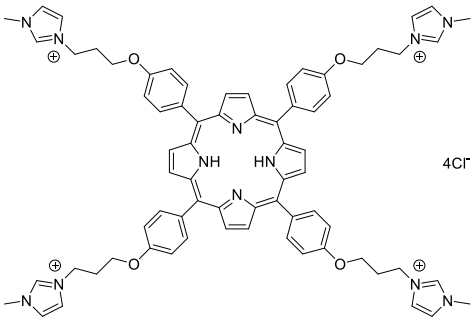

Compound 2. To a solution of **S5** (18 mg, 0.016 mmol) in 1-methylimidazole (2 mL), N_2 was bubbled for 10 min. The reaction mixture was stirred at 80 °C for 14 h, and then cooled to room temperature. The reaction mixture was concentrated *in vacuo* and the residue was dissolved in MeOH and precipitated by Et_2O. The solvent was decanted off and the precipitate was washed with Et_2O multiple times. The crude mixture was purified by a reverse phase HPLC (column: column: YMC-Pack ODS-A F20 mm x 250 mm; solvents MeCN-H_2O (10% to 40% MeCN containing 0.1% TFA gradient over 30 min) to provide compound **2** in a TFA salt form. The product was stirred overnight with DOWEX 1x8-200 resin (5 g) in water (10 mL) to have chloride as a counter anion. The mixture was filtered on sintered glass and the filtrate was concentrated *in vacuo*, lyophilized, and analyzed by HPLC to confirm the purity, to provide compound **2** as green fluffy solids (16 mg, 0.012 mmol, y = 75%); mp > 300 °C; FT-IR (ATR) υ_{max} (cm^{-1}): 3380, 3315, 3153, 3096, 2914, 2868, 1674, 1603, 1562, 1507, 1467, 1416, 1392, 1348, 1284, 1241, 1196, 1165, 1116, 1074, 1049, 1013,

983, 964, 827, 801, 743, 665, 622; ^{1}H-NMR (400 MHz, DMSO-d_6) δ_H –2.89 (br s, 2H, inner N-**H**), 2.52 (8H, CH_2-C**H$_2$**-CH_2, overlapping with DMSO), 3.93 (s, 12H, N-C**H3**), 4.36 (t, J = 5.8 Hz, 8H, CH_2-C**H$_2$**-N), 4.54 (t, J = 7.0 Hz, 8H, Ar-O-C**H$_2$**-CH_2), 7.37 (d, J = 8.7 Hz, 8H, Ph-**H**, *meta* to porphyrin), 7.82 (t, J = 1.6 Hz, 4H, imidazole 4'C-**H**), 7.96 (t, J = 1.6 Hz, 4H, imidazole 5'C-**H**), 8.13 (d, J = 8.6, 8H, Ar-**H**, *ortho* to porphyrin), 8.86 (s, 8H, β-pyrrole-**H**), 9.34 (s, 4H, imidazole 2'C-**H**); ^{13}C-NMR (100 MHz, DMSO-d_6) δ 29.92 (CH_2-**C**H_2-CH_2) 36.45 (imidazole, N-**C**H3). 47.22 (O-**C**H_2-CH_2), 65.55 (CH_2-**C**H_2-N), 113.63 (Ar-**C**, *meta* to porphyrin), 123.21 (imidazole 5'**C**), 124.34 (imidazole 4'**C**), 131.43 (broad, β-pyrrole **C**), 134.34 (Ar**C**, *ipso* to porphyrin), 136.01 (Ar**C**, *ortho* to porphyrin), 137.57 (imidazole 2'**C**), 158.82 (Ar**C**, *para* to porphyrin); HRMS (ESI$^+$) *m/z* calcd. for $C_{72}H_{74}N_{12}O_4^{4+}$: 292.6484, found: 292.6485 (M^{4+}).

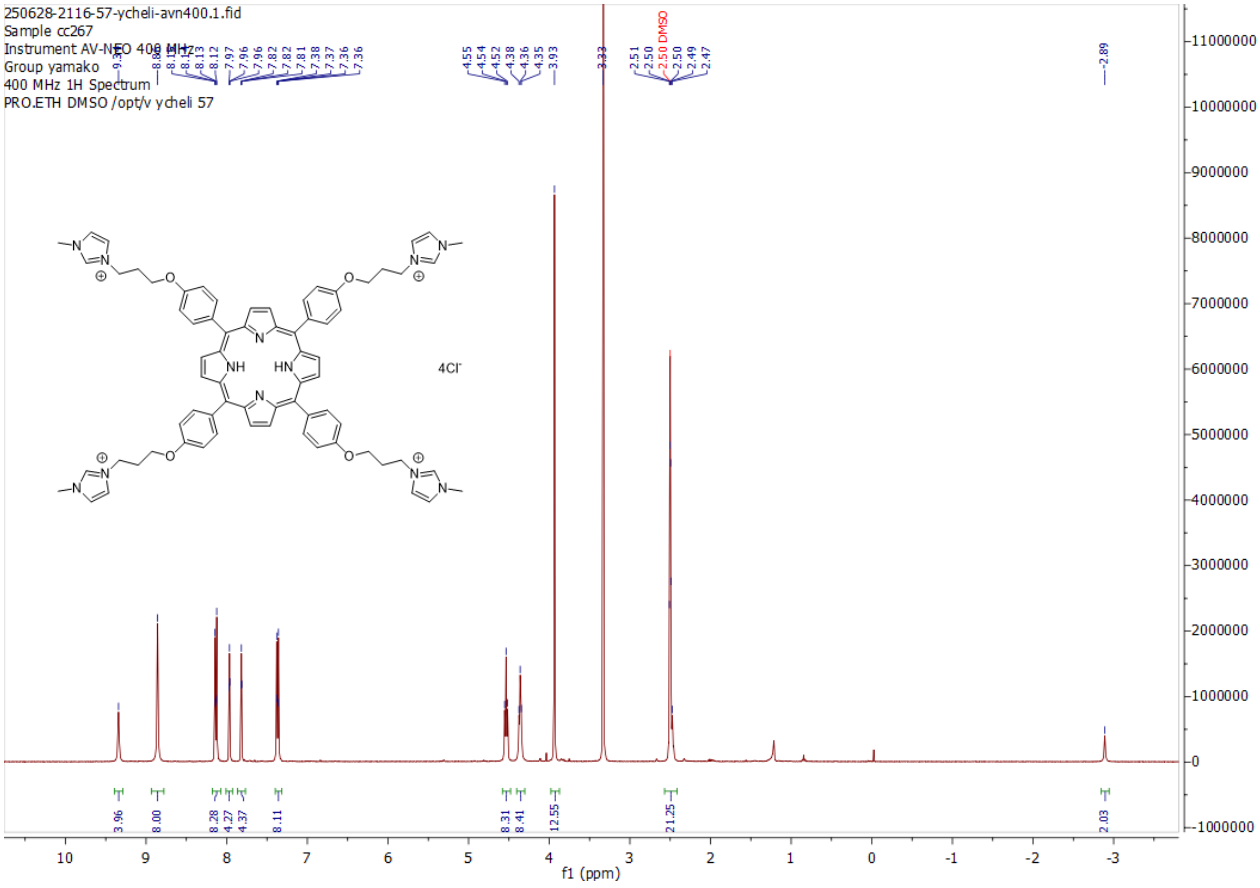

Fig. S18. ^{1}H-NMR spectrum of **2** (400 MHz, DMSO-d_6).

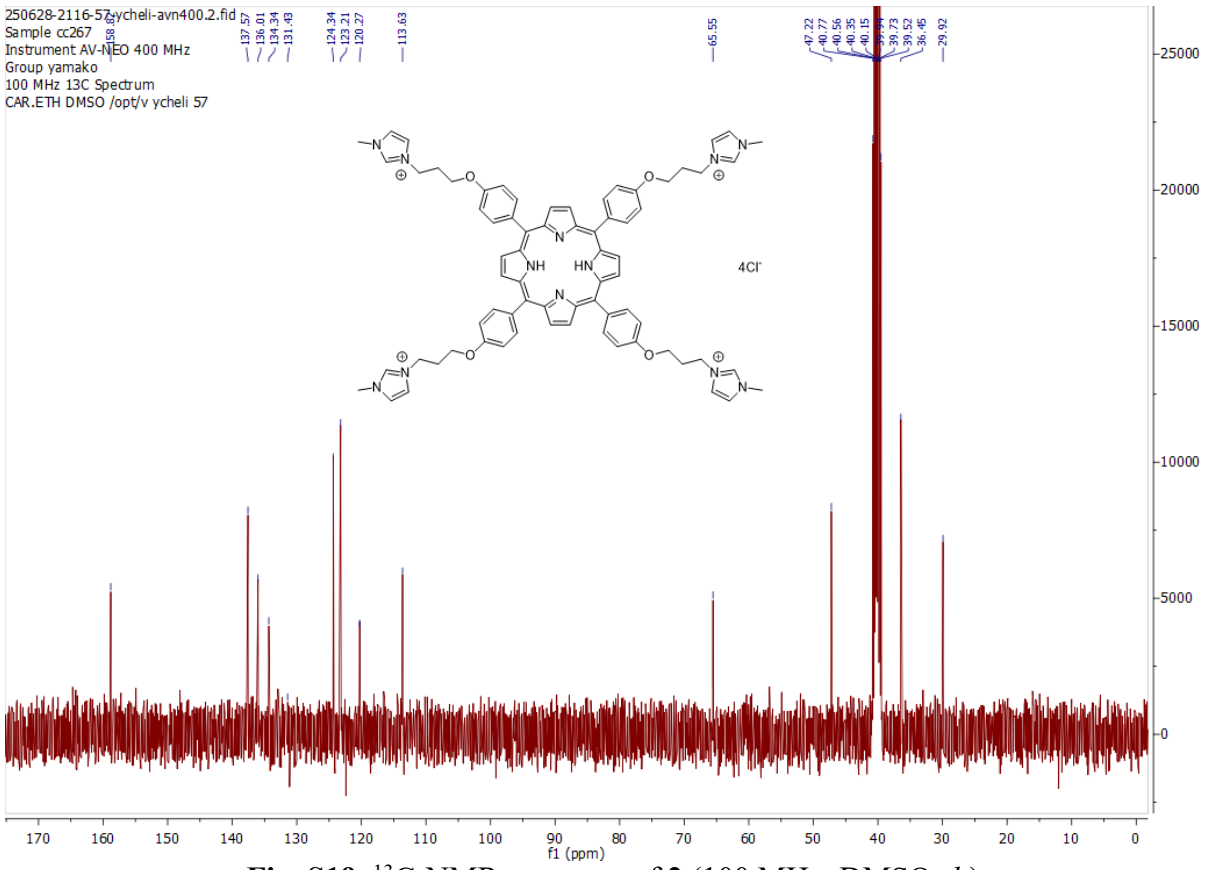

Fig. S19. ^{13}C-NMR spectrum of **2** (100 MHz, DMSO-d_6).

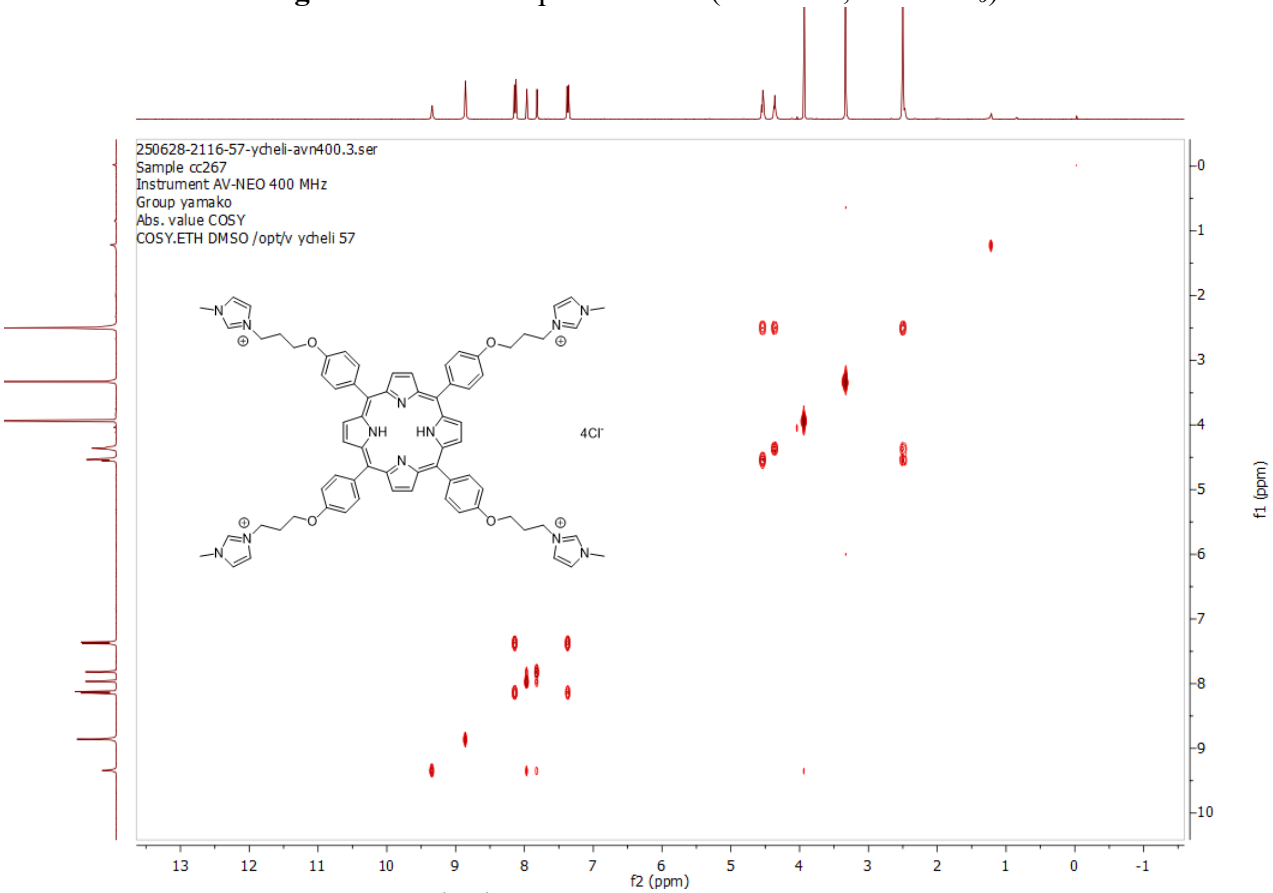

Fig. S20. ^{1}H/^{1}H COSY spectrum of **2** (DMSO-d_6).

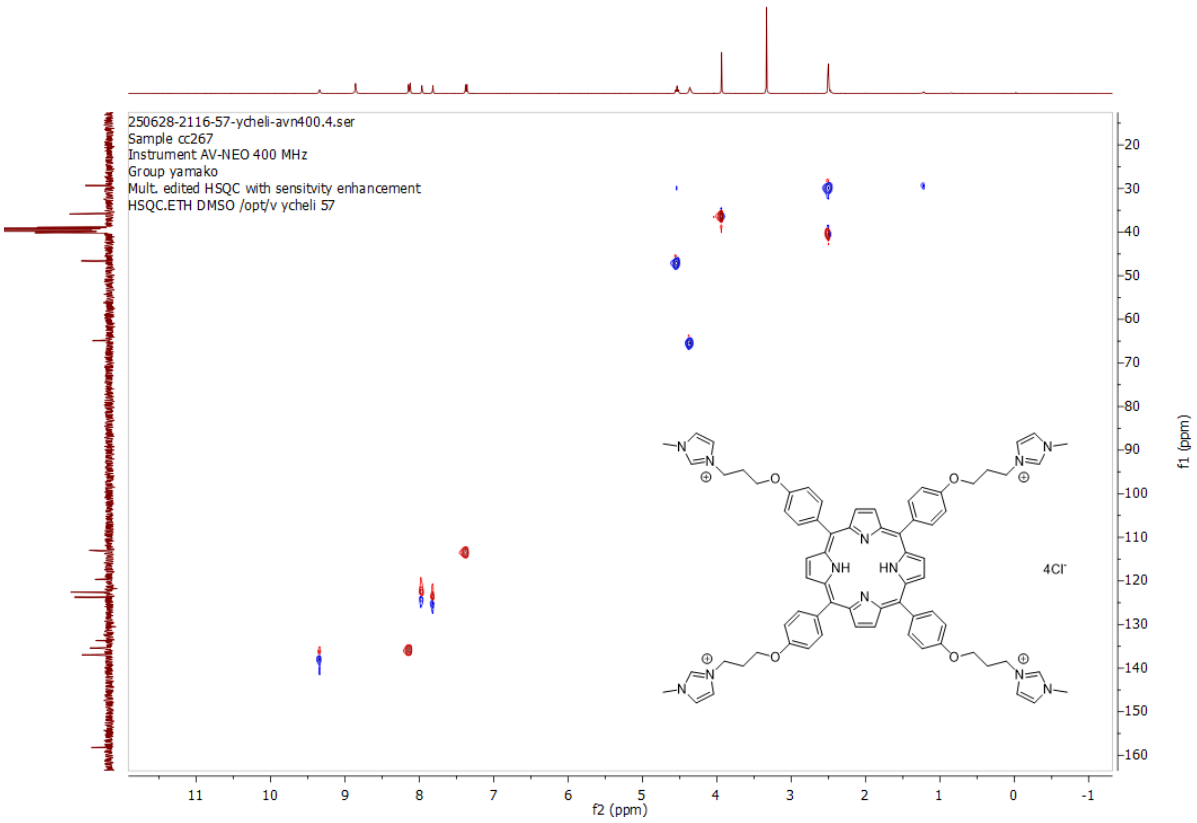

Fig. S21. HSQC-NMR spectrum of **2** (DMSO-d_6).

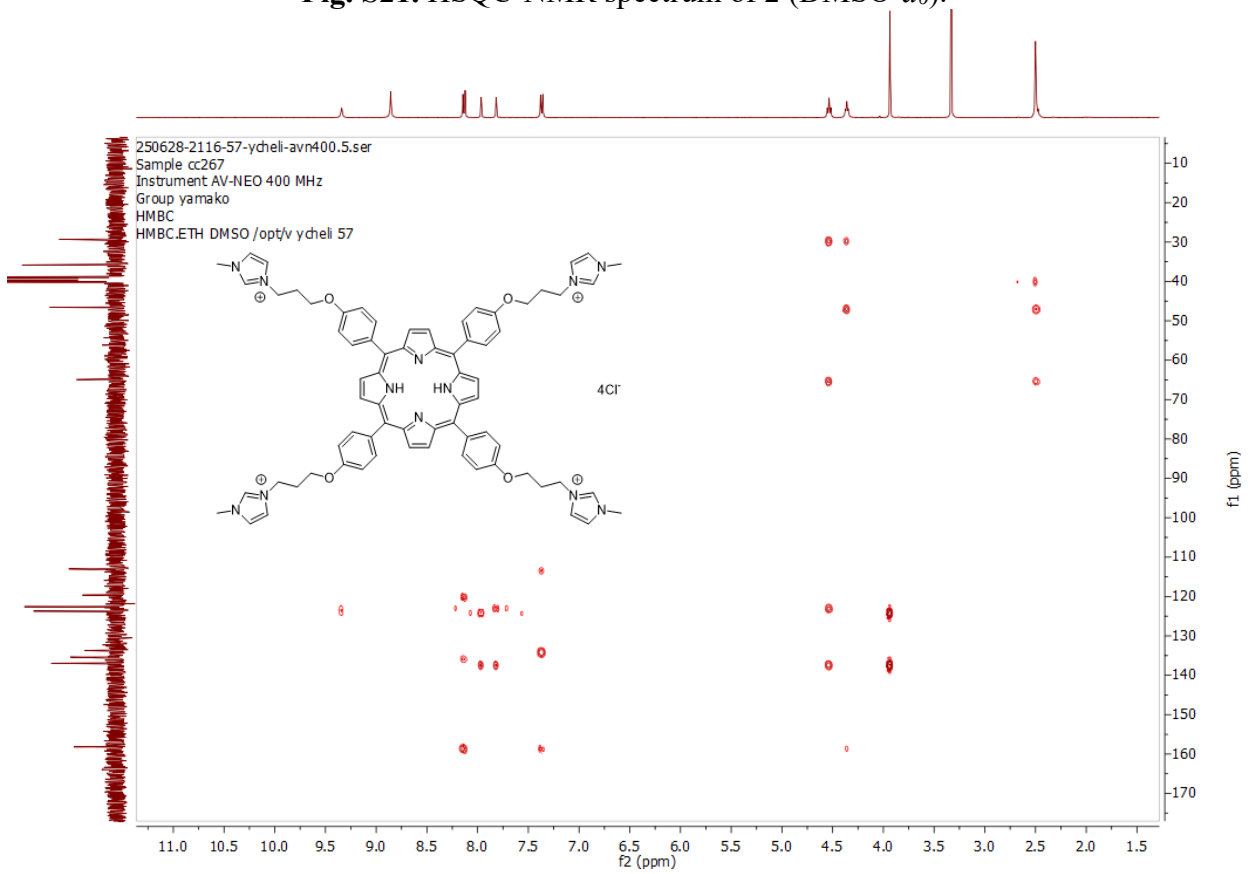

Fig. S22. HMBC-NMR spectrum of **2** (DMSO-d_6).

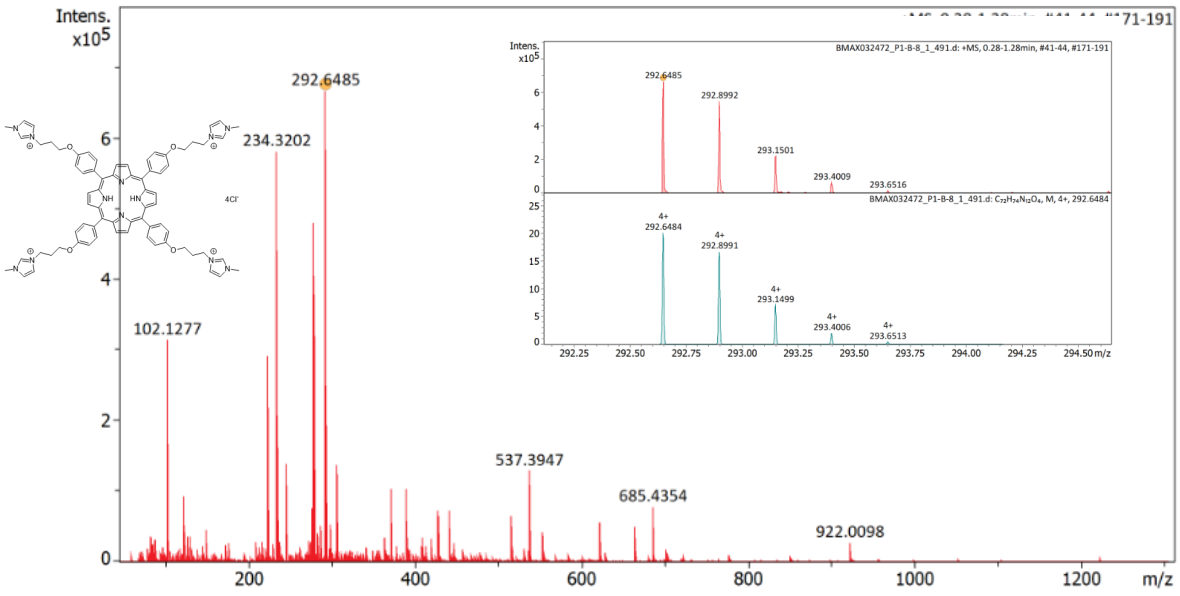

Fig. S23. Measured (inset top) and simulated (inset bottom) HR-ESI-MS spectra of **2**.

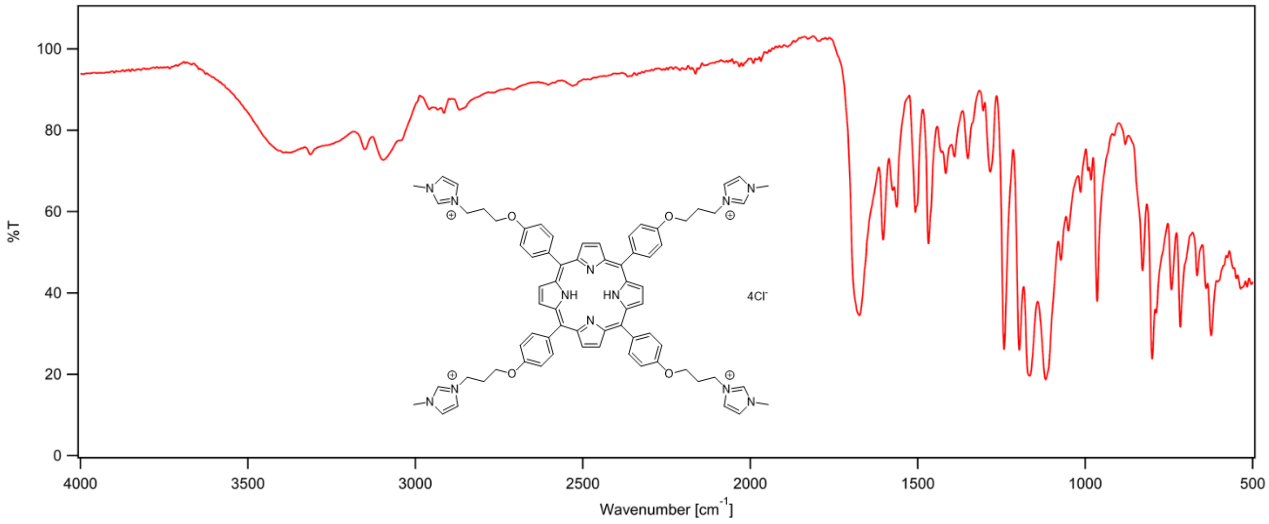

Fig. S24. FT-IR ATR spectrum of **2**.

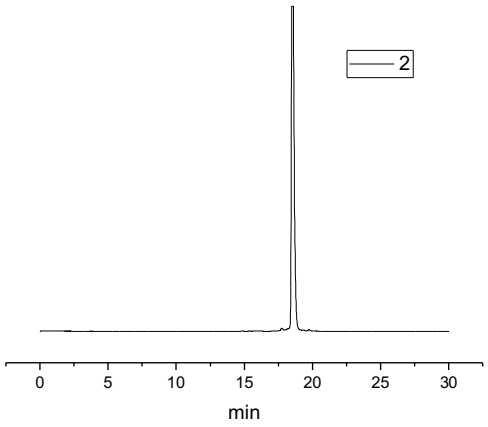

Fig. S25. RP-HPLC chromatogram of **2** (Column: Shiseido Capcell Pack C18 (4.6 mm x 250 mm); solvents: H_2O - MeCN (90:10 for 3 min, gradient to 10:90 over 22 min, then 10:90 for 5 min); flow rate: 1 mL•min^{-1}; detection: 220 nm.)

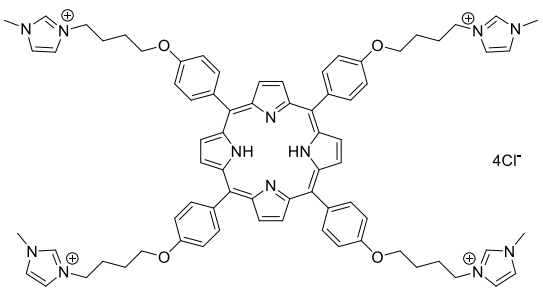

Compound 3. To a solution of **S6** (150 mg, 0.12 mmol) in 1-methylimidazole (10 mL), N_2 was bubbled for 10 min. The reaction mixture was stirred at 80 °C for 14 h, and then cooled to room temperature. The reaction mixture was concentrated *in vacuo* and the residue was dissolved in MeOH and precipitated by Et_2O. The solvent was decanted off and the precipitate was washed with Et_2O multiple times. The crude mixture was purified by a reverse phase HPLC (column: column: YMC-Pack ODS-A F20 mm x 250 mm; solvents MeCN-H_2O (10% to 40% MeCN containing 0.1% TFA gradient over 30 min) to provide compound **3** in a TFA salt form. The product was stirred overnight with DOWEX 1x8-200 resin (5 g) in water (10 mL) to have chloride as a counter anion. The mixture was filtered on sintered glass and the filtrate was concentrated *in vacuo*, lyophilized, and analyzed by HPLC to confirm the purity, to provide compound **3** as green fluffy solids (95 mg, 0.06 mmol, y = 45%); mp > 300 °C; FT-IR (ATR) υ_{max} (cm^{-1}): 3406, 3315, 3153, 3097, 2948, 2872, 1672, 1603, 1572, 1505, 1468, 1412, 1348, 1281, 1240, 1198, 1168, 1119, 1068, 1020, 981, 964, 879, 825, 798, 735, 717, 620; ^{1}H-NMR (400 MHz, DMSO-d_6) δ_H –2.88 (br s, 2H, inner N-**H**), 1.92 (m, 8H, O-CH_2-**CH_2-**CH_2), 2.15 (m, 8H, CH_2-**CH_2-**CH_2-N), 3.93 (s, 12H, N-C**H3**), 4.32 (t, *J* = 6.1 Hz, 8H, CH2-C**H**2-N), 4.40 (t, *J* = 7.1 Hz, 8H, Ar-O-C**H**$_2$-CH_2), 7.39 (d, *J* = 8.7 Hz, 8H, Ph-**H**, *meta* to porphyrin), 7.80 (t, *J* = 1.8 Hz, 4H, imidazole 4'C-**H**), 7.92 (t, *J* = 1.8 Hz, 4H, imidazole 5'C-**H**), 8.13 (d, *J* = 8.6, 8H, Ar-**H**, *ortho* to porphyrin), 8.87 (s, 8H, β-pyrrole-**H**), 9.30 (s, 4H, imidazole 2'C-**H**); ^{13}C-NMR (100 MHz, DMSO-d_6) δ 25.79 (O-CH_2-**C**H_2-CH_2), 26.77 (CH_2-**C**H_2-CH_2-N), 36.02 (imidazole, N-**C**H3), 48.85 (O-**C**H_2-CH_2), 67.33 (CH_2-**C**H_2-N), 113.21 (Ar-**C**, *meta* to porphyrin), 122.60 (imidazole 5'**C**), 123.97 (imidazole 4'**C**), 131.43 (broad, β-pyrrole **C**), 133.73 (Ar**C**, *ipso* to porphyrin), 135.60 (Ar**C**, *ortho* to porphyrin), 136.97 (imidazole 2'**C**), 158.70 (Ar**C**, *para* to porphyrin); HRMS (ESI^+) *m/z* calcd. for $C_{72}H_{74}N_{12}O_4^{4+}$: 306.6640, found: 306.6641 (M^{4+}).

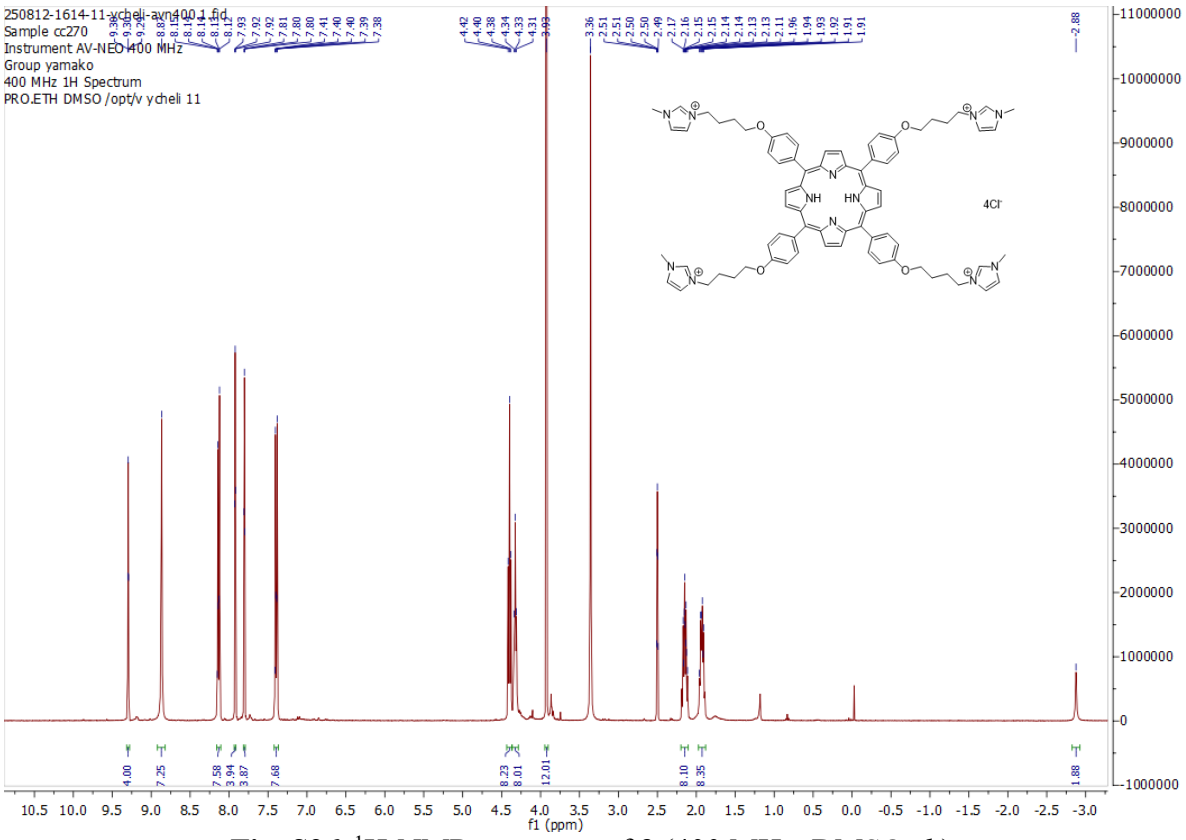

Fig. S26. ^{1}H-NMR spectrum of **3** (400 MHz, DMSO-d_6).

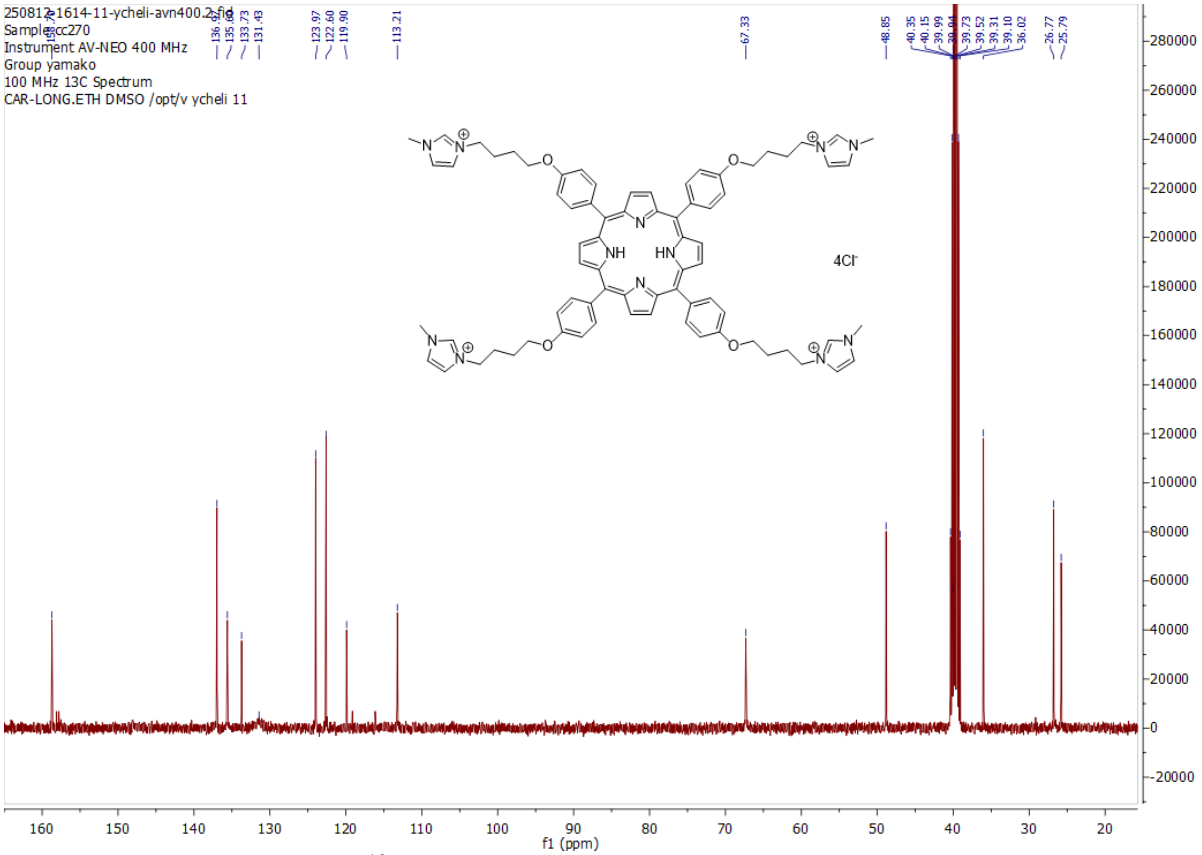

Fig. S27. ^{13}C-NMR spectrum of **3** (100 MHz, DMSO-d_6).

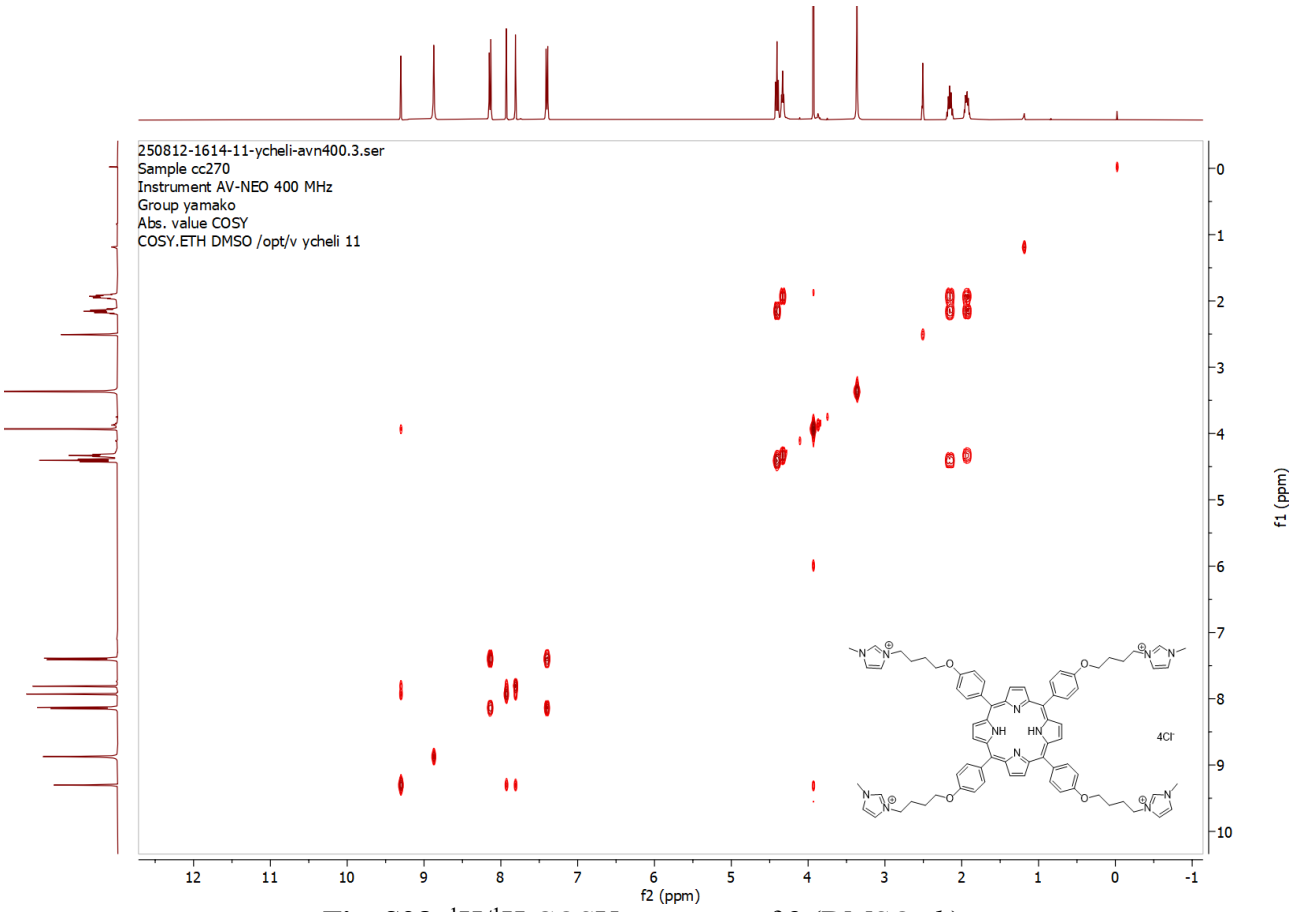

Fig. S28. $^{1}H/^{1}H$ COSY spectrum of **3** (DMSO-d_6).

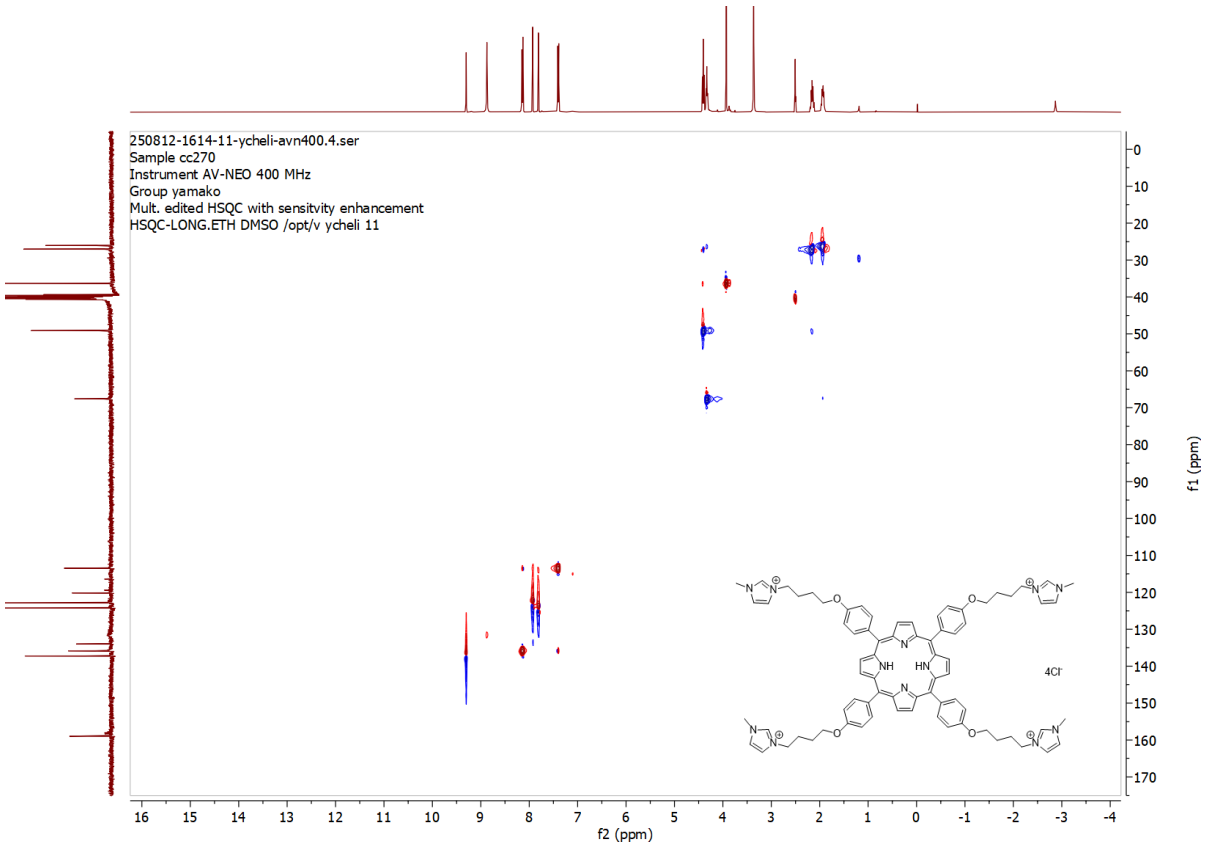

Fig. S29. HSQC-NMR spectrum of **3** (DMSO-d_6).

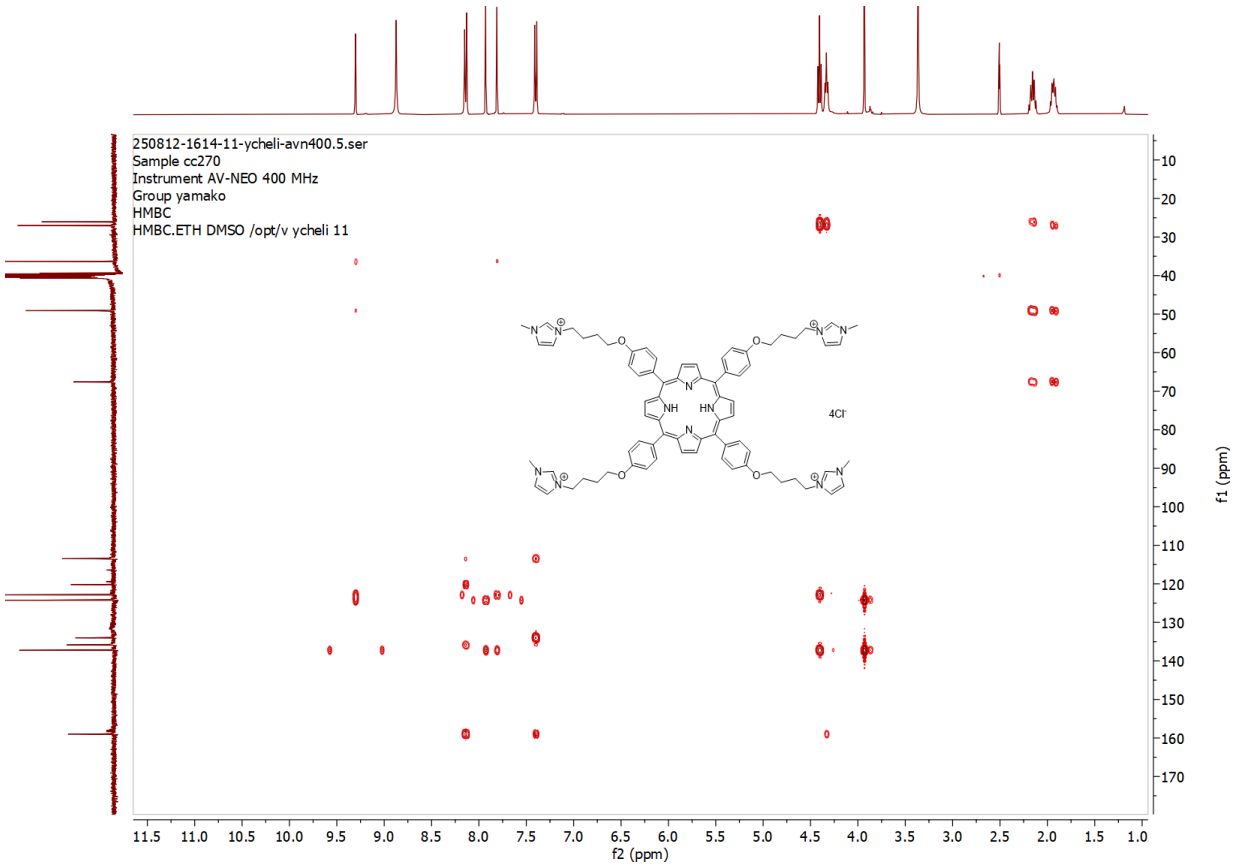

Fig. S30. HMBC-NMR spectrum of **3** (DMSO-d_6).

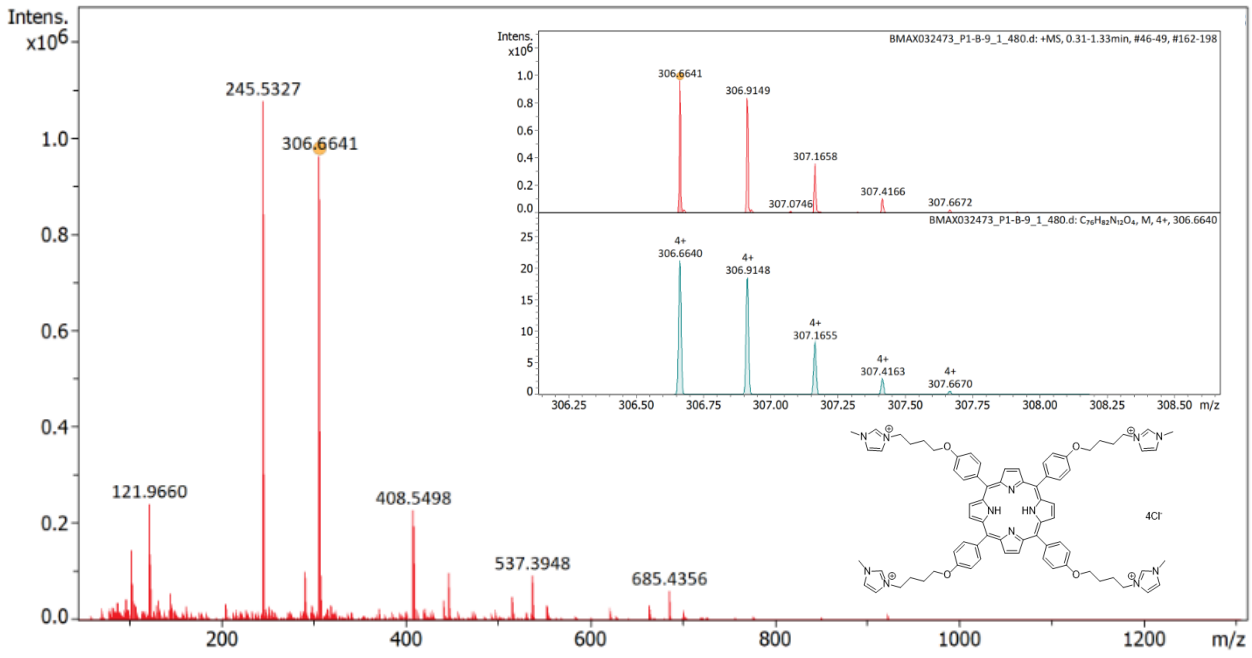

Fig. S31. Measured (inset top) and simulated (inset bottom) HR-ESI-MS spectra of **3**.

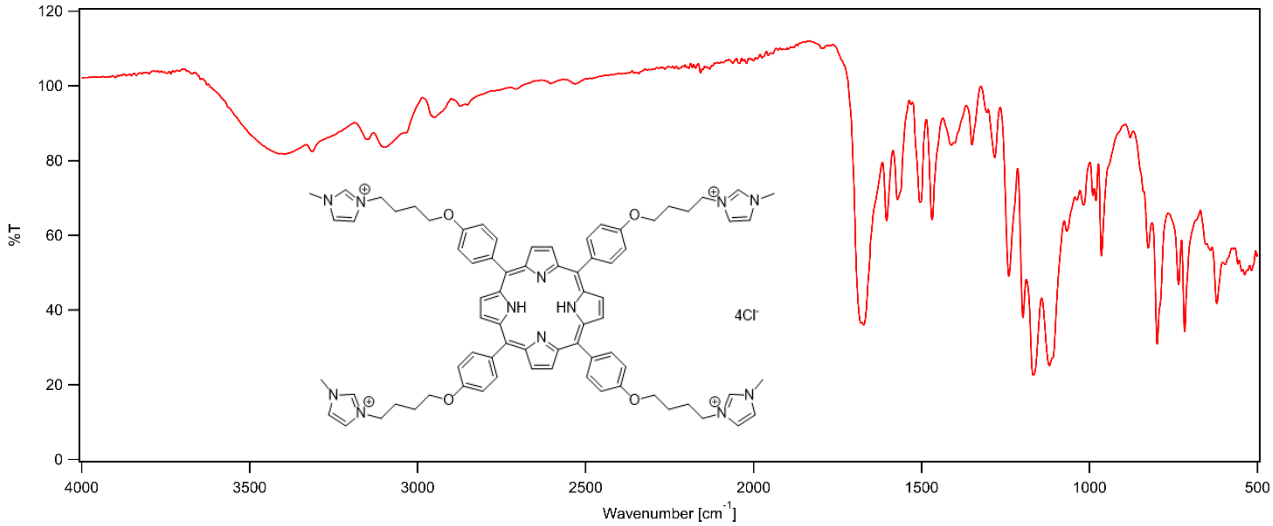

Fig. S32. FT-IR ATR spectrum of **3**.

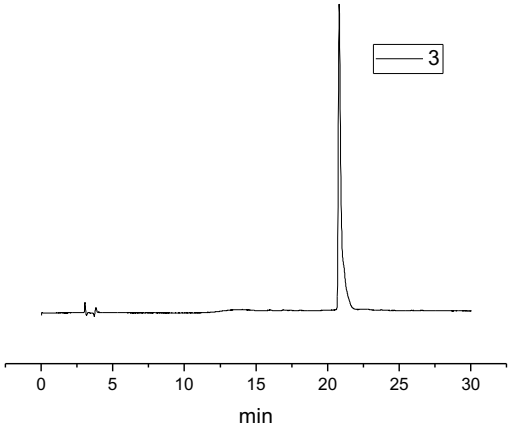

Fig. S33. RP-HPLC chromatogram of **3** (Column: Shiseido Capcell Pack C18 (4.6 mm x 250 mm); solvents: H_2O - MeCN (90:10 for 3 min, gradient to 10:90 over 22 min, then 10:90 for 5 min); flow rate: 1 mL•min^{-1}; detection: 220 nm.)

2. UV-Vis measurements

Absorption spectra were recorded on a JASCO V-570 UV/VIS/NIR spectrophotometer (JASCO Co., Tokyo, Japan). DNA oligonucleotides were purchased from Integrated DNA Technologies, Inc. (Coralville, IA, USA). Each solution of **1**, **2**, or **3** (5 µM) was prepared in 10 mM HEPES buffer (pH 7.4, containing 100 mM KCl and 1 mM Na_2EDTA). A solution of single strand telo24 DNA (500 µM) with the sequence of d(TTAGGGTTAGGGTTAGGGTTAGGG) was prepared in same buffer and subjected to the pre-annealing process by heating at 90 °C for 10 min and cooling back to room temperature over 3 hours. Similarly, hairpin DNA with the sequence of d(CGAATTCGTCTCCGAATTCG) was prepared in the same buffer. To each porphyrin solution (2 mL) in a quartz UV cuvette (path length: 1 cm), an aliquot of the DNA solution was added and left to equilibrate for 2 min upon mixing to record UV-vis spectra. The titration was stopped when there was no change observed upon three consecutive additions of DNA. Binding data were plotted and analyzed using the equation below[1]

$$\frac{[DNA]}{\Delta\varepsilon_{ap}} = \frac{1}{\Delta\varepsilon}[DNA] + \frac{1}{\Delta\varepsilon K_a}$$

where [*DNA*] is the concentration of DNA in the solution, $\Delta\varepsilon_{ap}$ is given by $\Delta\varepsilon_{ap} = \varepsilon_f - \varepsilon$; where ε_f is the extinction coefficient of the free ligand and ε is the observed extinction coefficient and Δε was given by $\Delta\varepsilon = \varepsilon_f - \varepsilon_b$ where ε_b is extinction coefficient of the fully bound ligand. Soret band maximum of each porphyrin was used for the analysis. Data were analyzed using GraphPad Prism 8.0.1 (GraphPad Software Inc., Boston, MA, USA) plotting [DNA]/$\Delta\varepsilon_{ap}$ vs [DNA] with linear regression. K_a values were calculated by the ratio of slope to the y intercept of the obtained graphs. K_d values were obtained by the relation of $K_a = 1/ K_d$. Hypochromicity values of the Soret band of the porphyrins were calculated by the formula percent hypochormicity = $[(\varepsilon_f - \varepsilon_b)/ \varepsilon_f]$ 100, where $\varepsilon_b = A_b/C_b$.

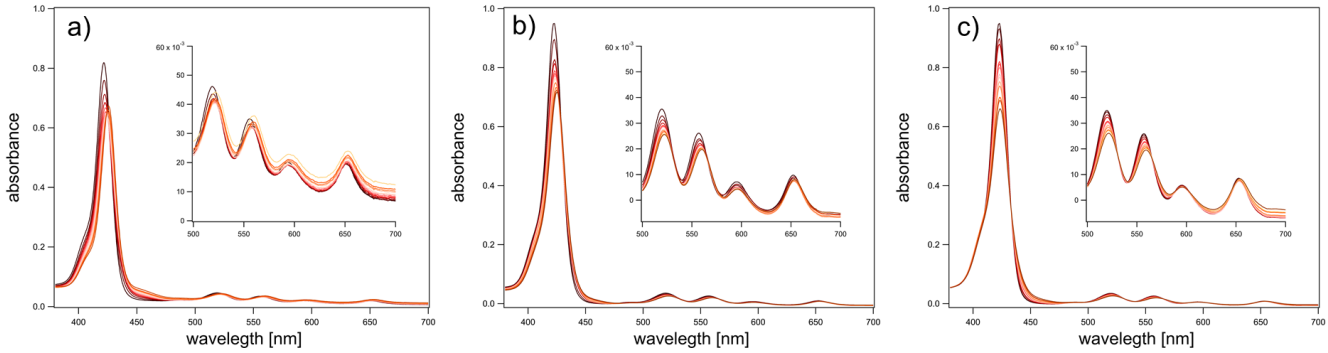

Fig. S34. UV-vis spectra of 5 μM solutions of compounds **1** (a), **2** (b) and **3** (c) in the presence of telo24 G4 DNA in 10 mM HEPES pH 7.4.

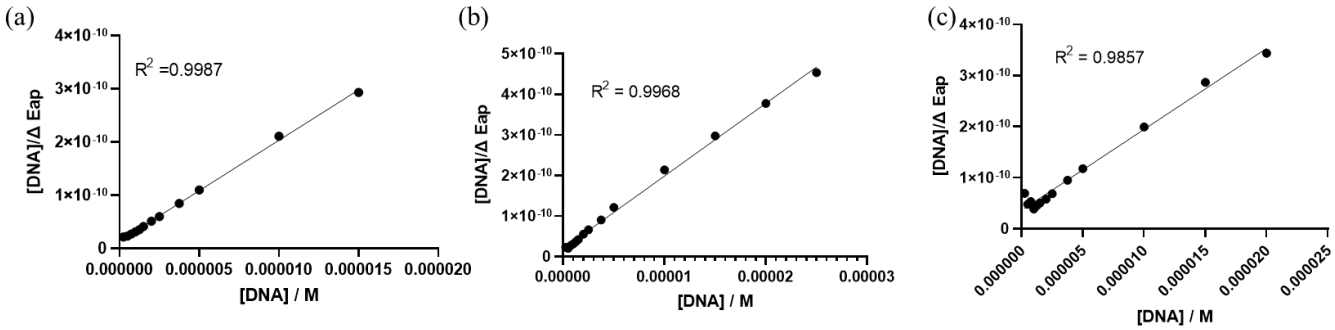

Fig. S35. Plots of [DNA]/$\Delta\varepsilon_{ap}$ vs [DNA] obtained from the titration of telo24 G4 DNA into compounds **1** (a), **2** (b) and **3** (c).

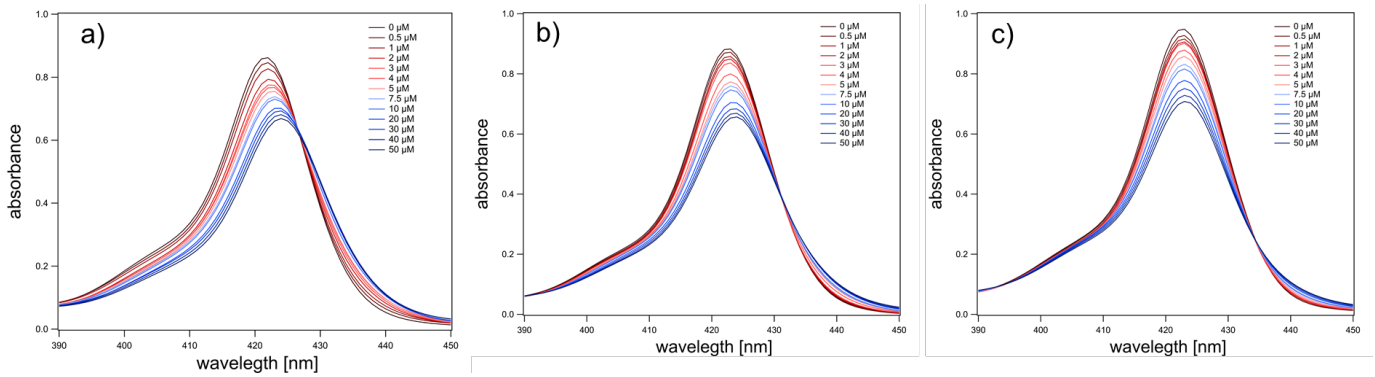

Fig. S36. UV-vis spectra of 5 µM compounds **1** (a), **2** (b) and **3** (c) near Soret band in the presence of hp DNA.

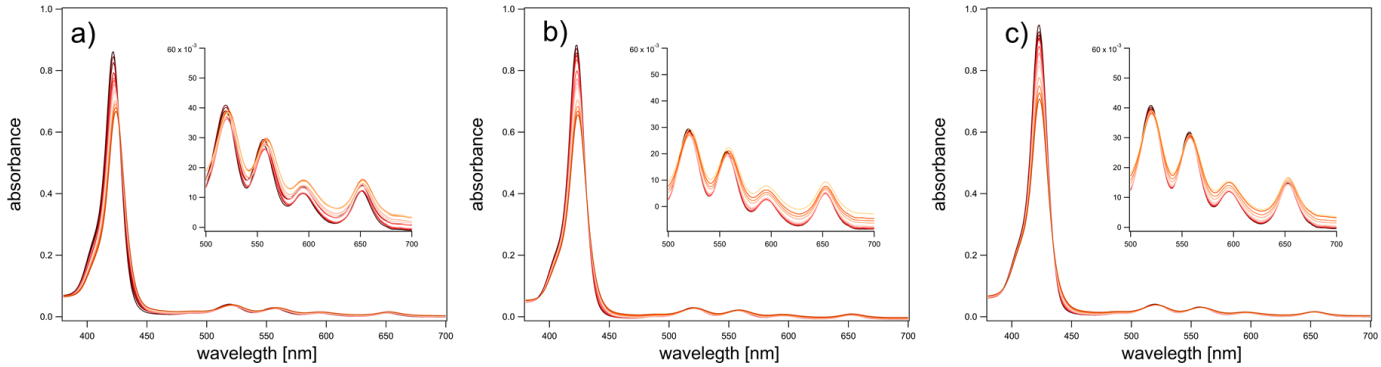

Fig. S37. UV-vis spectra of 5 µM solutions of compounds **1** (a), **2** (b) and **3** (c) in the presence of hpDNA in 10 mM HEPES pH 7.4.

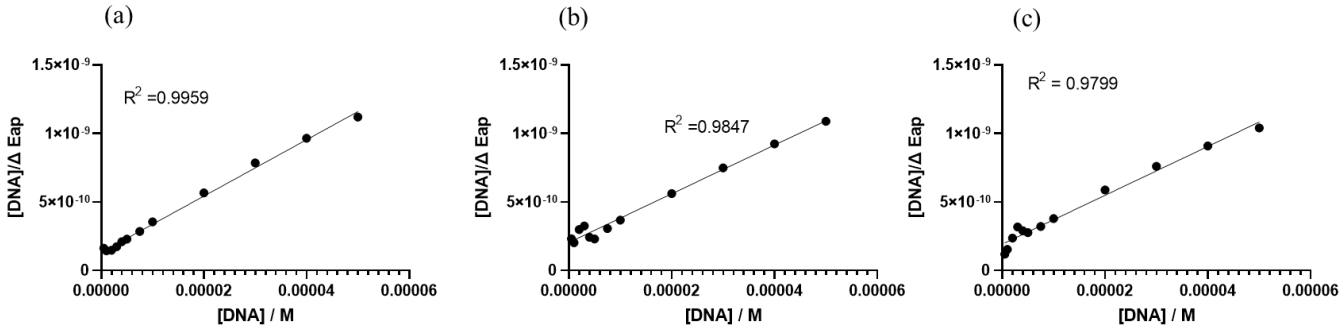

Fig. S38. Plots of [DNA]/$\Delta\varepsilon_{ap}$ vs [DNA] obtained from the titration of hpDNA into compounds **1** (a), **2** (b) and **3** (c).

3. FRET melting assay

3.1 FRET melting assay for G4 stabilization effect

G4 stabilization effects of the porphyrins were evaluated using FRET melting assay with telo24 and Rif1-2 as G4 DNA. Dual-labeled oligonucleotides, modified with 6-carboxyfluorescein (FAM) at 5'- end and tetramethyl-rhodamine (TAMRA) at 3'-end, were purchased from Fasmac Co., Ltd. (Kanagawa, Japan). The sequences used were as follows:

telo24: 5'-FAM-TTAGGGTTAGGGTTAGGGTTAGGG-TAMRA-3'

Rif1-2: 5'-FAM-AAGGCAATGTGGGGGGATAGTGGGCA- TAMRA-3'.

G4 folding and FRET measurements were performed according to previously described procedure.[2] Briefly, the single-stranded G4 DNA probes at 0.4 μM in the 1× FRET Buffer (10 mM lithium cacodylate, 1 mM KCl, 99 mM lithium chloride) were denatured at 95 °C for 5 min, followed by gradual cooling to room temperature on the heat block over 2 h to allow quadruplex formation. Subsequently, G4 DNA (final concentration: 0.2 μM) was mixed with varying concentrations (0.16, 0.3, 0.6, 1.3, 2.5, 5, and 10 μM) of each porphyrin in 1× FRET Buffer (total 40 μL). FAM fluorescence emission was monitored from 25 °C to 99 °C with a ramp speed of 1 °C per min using a CFX96 and C-1000 real-time PCR detection system (Bio-Rad) with excitation at 450–480 nm and detection at 510–530 nm. The melting temperature (T_m) was defined as the temperature at which the normalized fluorescence intensity reached 50%. For this calculation, the maximum and minimum fluorescence intensities in the absence of compounds (at 99 °C and 25 °C, respectively) were normalized to 100% and 0%. The change in melting temperature (ΔT_m) resulting from porphyrin addition was calculated using the following equation to assess G4 stabilization ability:

$$\Delta T_m = T_{m\,(x,\,y)} - T_{m\,min}$$

where $T_{m\,(x,\,y)}$ is the Tm of G4 probe in the presence of the compound x at concentration y. $T_{m\,min}$ is the melting temperature in the absence of the compound.

Table S1. The melting temperature (T_m) of telo24 G4 DNA in presence of the porphyrins. The T_m values of telo24 G4 DNA were determined in presence of the compound **1**, **2**, **3** or **TMPyP4** at various concentrations. The change in melting temperature (ΔT_m) was calculated as the difference between the Tm value in the presence of each compound and the Tm value in the absence of compounds (control; presented as concentration '0').

	Porphyrins	Concentration of porphyrins [μM]							
		0	0.16	0.3	0.6	1.3	2.5	5	10
T_m	**1**	41	37	73	93	99<	99<	99<	99<
	2	41	33	35	37	63	89	99<	99<
	3	41	33	48	69	99<	99<	99<	99<
	TMPyP4	41	60	76	91	99<	99<	99<	99<
ΔT_m	**1**	0	-4	32	52	59<	59<	59<	59<
	2	0	-8	-6	-4	22	48	59<	59<
	3	0	-8	7	28	59<	59<	59<	59<
	TMPyP4	0	19	35	50	59<	59<	59<	59<

Table S2. Melting temperature (T_m) of Rif1-2 G4 DNA in presence of the porphyrins.

	Porphyrins	Concentration of porphyrins [μM]							
		0	0.16	0.3	0.6	1.3	2.5	5	10
T_m	**1**	35	31	81	99<	99<	99<	99<	99<
	2	35	26	28	31	67	99<	99<	99<
	3	35	34	44	88	99<	99<	99<	99<
	TMPyP4	35	31	99<	99<	99<	99<	99<	99<
ΔT_m	**1**	0	-4	46	65<	65<	65<	65<	65<
	2	0	-9	-7	-4	32	65<	65<	65<
	3	0	-1	9	53	65<	65<	65<	65<
	TMPyP4	0	-4	65<	65<	65<	65<	65<	65<

3. 2 Effect of competitors on G4 stabilization by porphyrin *via* FRET assay

To evaluate the structural selectivity of the porphyrins for G4 DNA, competitive FRET assays were performed. The G4 DNA (0.2 μM) was mixed with each compound (final concentration: 1.25 μM) in the presence of either a G4 or non-G4 DNA competitor (final concentrations: 5 or 15 μM) in 1× FRET buffer (total volume: 40 μL). The sequences of the competitors were as follows:

telo24 (G4), 5'- TTAGGGTTAGGGTTAGGGTTAGGG -3'

telo24 mut (non-G4), 5'- TTAAGATTAAGATTAAGATTAAGA -3'

Rif1-2 (G4), 5'- AAGGCAATGTGGGGGGATAGTGGGCA -3'

Rif1-2 mut (non-G4), 5'- AAGGCAATGTAGAGAGATAGTAGACA -3'

G4 competitors were folded using the same procedure as described for the G4 probes, while non-G4 competitors were used as single-stranded DNA (ssDNA). To quantify the destabilization effect of the competitors, FAM fluorescence signals were normalized using the following equation:

$$\text{Normalized FAM signal intensities} = (F_{(x,z)} - F_{min}) / (F_{max} - F_{min})$$

where $F_{(x,z)}$ represents the absolute FAM emission intensity in the presence of compound x and competitor z (Fig. S40). F_{min} is the minimum emission intensity in the presence of the compound without a competitor, and F_{max} is the maximum intensity in the absence of both compounds and competitors. Detailed Normalization Procedure was presented in Fig. S40. Because the competitive effect was dependent on both the compound and the temperature, we identified the specific temperature at which the difference in normalized FAM intensity between the G4 and non-G4 competitors was maximized for each compound ($Temp_{\Delta max}$). The normalized values at $Temp_{\Delta max}$ were then defined as the "G4 destabilization effect" (expressed as a percentage). Although assays were conducted at two different concentrations of the competitor, results at 5 μM of competitor are presented as representative data, as higher concentrations (15 μM) appeared to diminish the observed structural specificity.

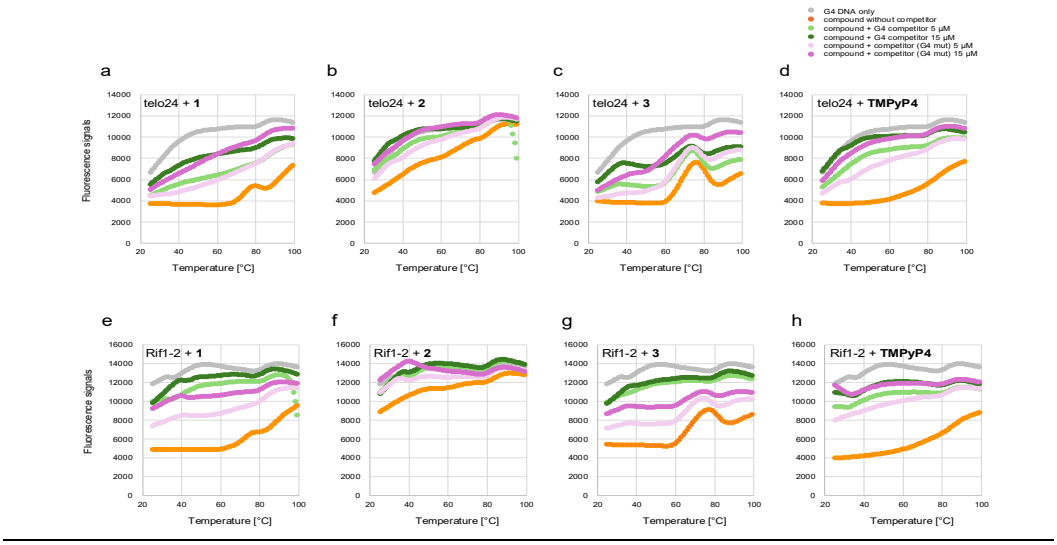

Fig. S39. Influence of G4 and non-G4 DNA competitors on the stabilization of G4 structures by porphyrins. Fluorescence emission spectra of telo24 (a–d) or Rif1-2 (e-h) G4 DNA (0.2 µM) were recorded in the presence of the compounds **1**, **2**, **3** or TMPyP4 (1.25 µM). Competitor G4 DNA (G4) or its mutant (non-G4; G4 mut) was added at concentrations of 5 µM or 15 µM as indicated. The plots represent the absolute fluorescence emission intensities as a function of temperature.

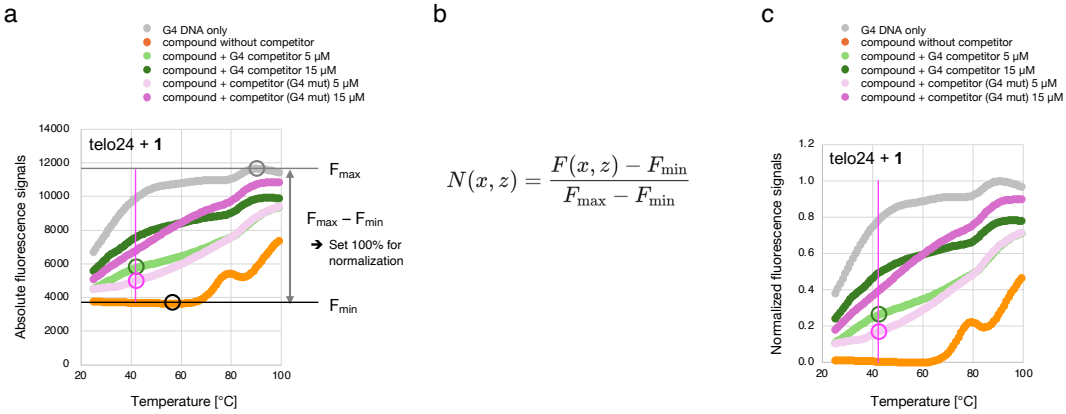

Fig. S40. Influence (a) Definition of parameters using absolute FAM fluorescence data. To ensure a quantitative comparison between different compounds, absolute fluorescence values (corresponding to Figure S39a) were normalized to a common scale. F_{max} (11,656; gray circle) was defined as the maximum fluorescence of telo24 G4 DNA at 90 °C in the absence of ligands, serving as a constant reference for the fully unfolded state across all telo24 G4 experiments. F_{min} was determined for each compound to account for baseline quenching effects; for compound 1, F_{min} was 3,630 at 58 °C (black circle). By defining these boundaries, the relative G4-stabilization effect can be measured independently of the initial fluorescence intensity. (b) Normalization Equation. This equation transforms raw intensity into a standardized metric of the unfolded state, where $F_{(x,z)}$ is the absolute intensity for compound (x) with competitor (z). This mathematical framework ensures that the resulting selectivity data are robust and suitable for quantitative inter-compound comparison. (c) Quantitative evaluation of G4-selectivity. Using the formula in b, absolute values were converted into a normalized ratio ranging from 0 to 1.0, allowing for a precise comparison of competitor impacts. At 42 °C ($Temp_{\Delta max}$; see Figure S42) the absolute values for the telo24 G4 competitor and its mutant in the presence of 1 were 5,737 (green circle in a) and 4,987 (magenta circle in a), respectively. These correspond to normalized values of 0.26 and 0.17 (circles in c). This normalization step is critical for calculating the "Selectivity Rate," as it provides a standardized metric to compare the structural preference of different porphyrins regardless of their varying quenching properties.

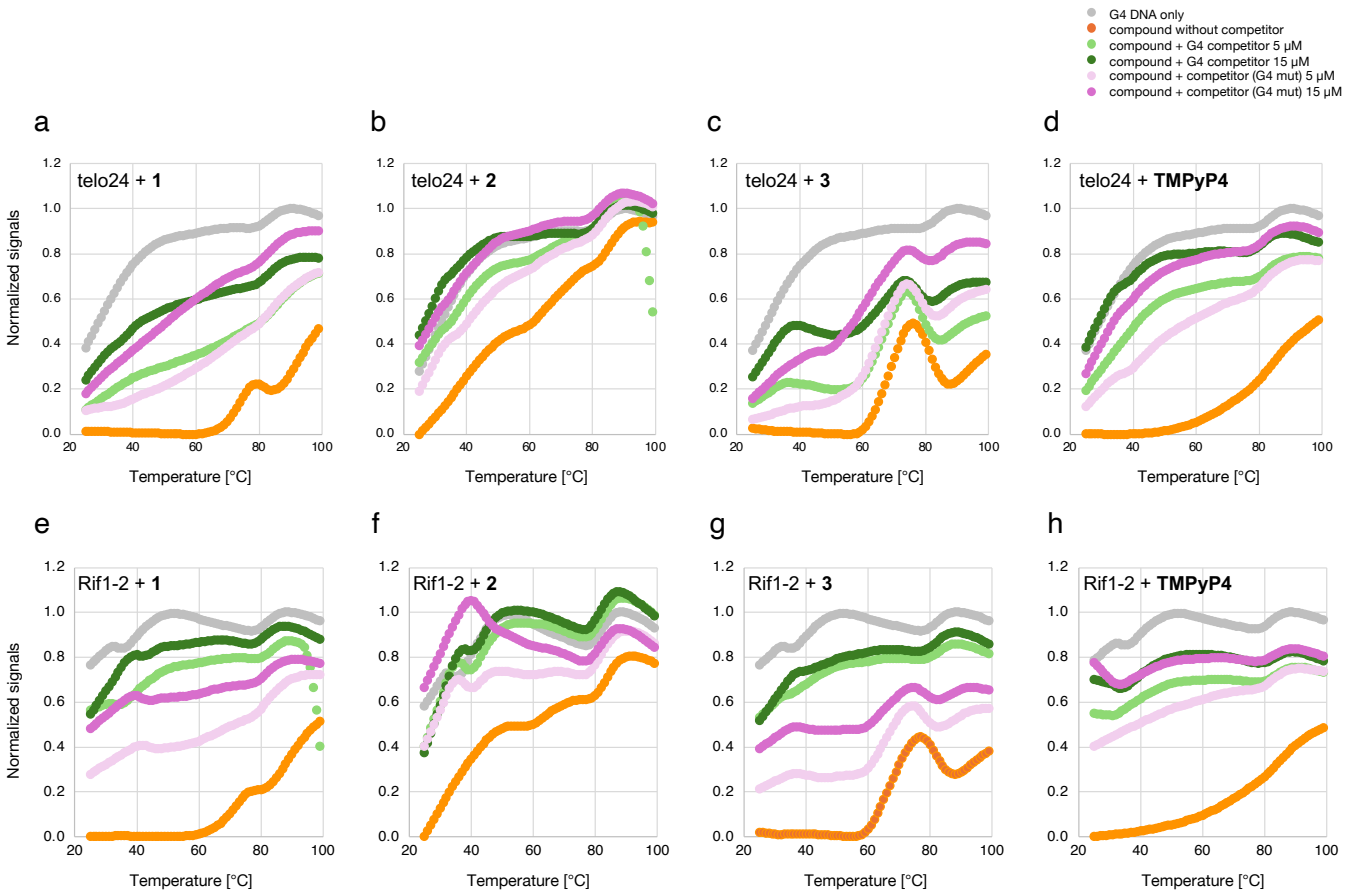

Fig. S41. Normalized FRET in competition assays for evaluating G4 stabilization specificity. The FAM fluorescence signals from Fig. S39 were normalized using the minimum values (recorded in the presence of compounds **1**, **2**, **3**, or TMPyP4 without competitors) and the maximum values (recorded in the absence of both compounds and competitors). Normalized signals for the telo24 (a–d) and Rif1-2 (e–h) G4 DNAs are shown. The Y-axis represents the relative destabilization of the G4 structure during the temperature shift (25–75 °C).

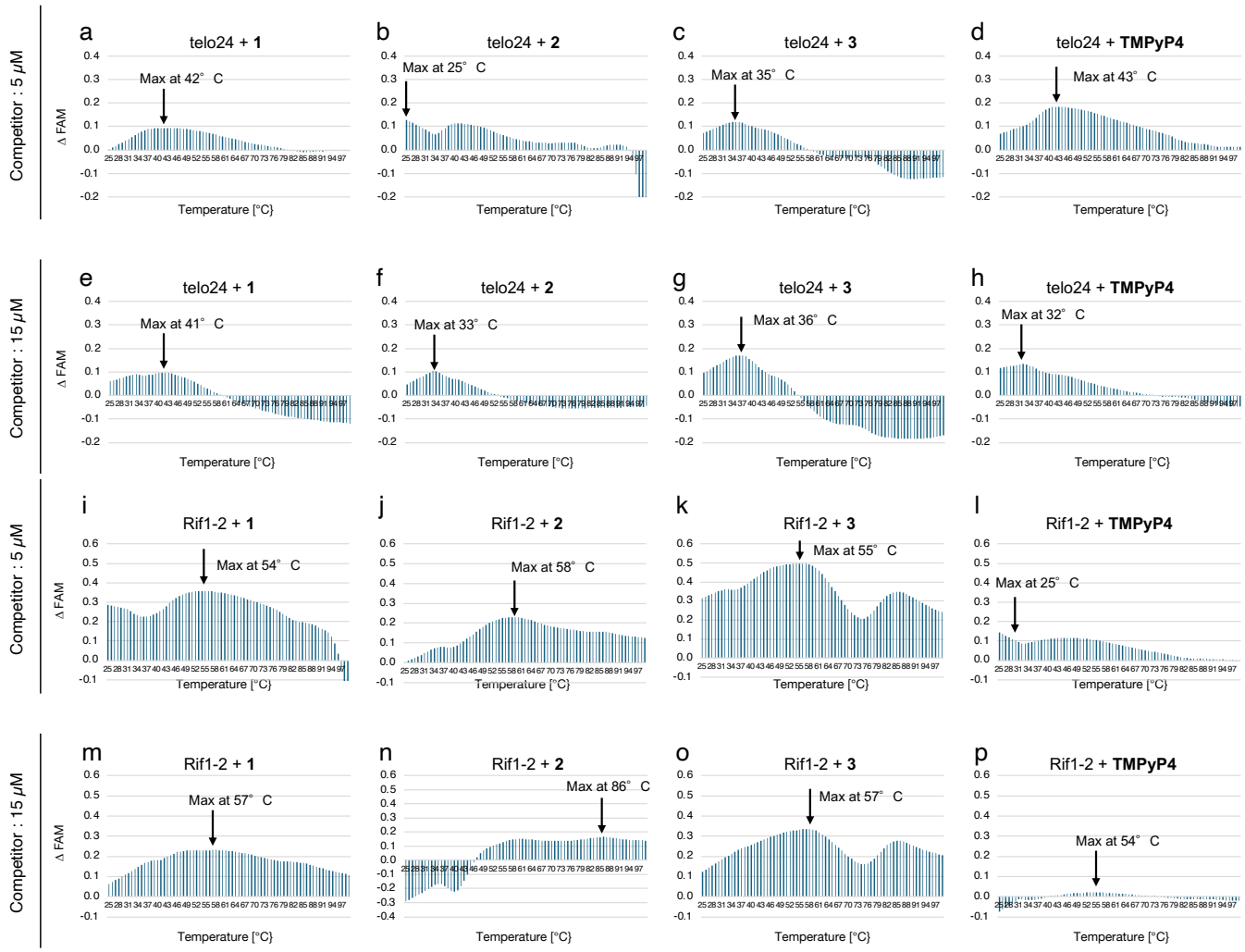

Fig S42. Temperature-dependent differences in G4 destabilization effects between G4 and non-G4 competitors. Normalized FAM signals for telo24 (a–h) and Rif1-2 (i–p) G4 DNAs were measured in the presence of compounds **1**, **2**, **3**, or **TMPyP4**, with the addition of either a G4 or non-G4 DNA competitor. Competitor concentrations were 5 μM (a–d and i–l) and 15 μM (e–h and m–p). The plots illustrate the calculated difference in normalized signals between the G4 and non-G4 competitors over a temperature range of 25–75 °C. Arrows indicate the temperature at which the maximum difference between the two competitors was observed ($Temp_{\Delta max}$), serving as the indicator for selectivity rate calculation.

Table S3. G4 selectivity rates of porphyrins for the telo24 G4 DNA. The selectivity rates were calculated as described in the legend for Fig. S41. The normalized FAM values at $Temp_{\Delta max}$ were plotted in Fig. 5c.

Competitor conc [μM]	$temp_{\Delta max}$ [°C]	Compounds	Normalized FAM values		Ratio G4/ mut
			Competitors		
			G4	G4 mut	
5	42	**1**	26	17	1.6
	25	**2**	32	19	1.7
	35	**3**	23	11	2.1
	43	TMPyP4	52	34	1.5
15	41	**1**	48	38	1.3
	33	**2**	68	58	1.2
	36	**3**	47	30	1.6
	32	TMPyP4	59	45	1.3

Table S4. G4 selectivity rates of porphyrins for the Rif1-2 G4 DNA probe. The selectivity rates were calculated as described in the legend for Fig. S41. Higher values indicate a greater preference of Rif1-2 for G4 topology over non-G4. The normalized FAM values at $Temp_{\Delta max}$ were plotted in Fig. 5d.

Competitor conc [μM]	$temp_{\Delta max}$ [°C]	Compounds	Normalized FAM values		Ratio G4/ mut
			Competitors		
			G4	G4 mut	
5	54	**1**	76	40	1.9
	58	**2**	95	72	1.3
	55	**3**	77	27	2.8
	25	TMPyP4	55	40	1.4
15	57	**1**	86	63	1.4
	86	**2**	108	92	1.2
	57	**3**	81	48	1.7
	54	TMPyP4	81	79	1.0

4. Photoinduced singlet oxygen generation

ESR spectra were recorded on a Bruker EMX, Continuous Wave X-Band EPR spectrometer (Bruker BioSpin GmbH). Each measurement was performed on the sampls in a Blaubrand® intraMark capillary (50 μL, Brand GMBH, Wertheim, Germany) placed inside a Suprasil® ESR tube (diameter: 4 mm, length: 250 mm, wall thickness: 0.8 mm; SP Wilmad-Lab Glass, NJ, USA). The 2,2,6,6-tetramethylpiperidin-4-one (4-oxo TEMP) was purchased from ABCR (Karlsruhe, Germany) and purified prior to use by sublimation. The 4-oxo-2,2,6,6-tetramethyl-1-piperidinyloxy (4-oxo TEMPO) was purchased from Sigma-Aldrich (St. Louis, Missouri, USA). Nunc MicroWell 96 Well Round (U) Bottom Plate was bought from Thermo Scientific (Waltham, MA, USA). Lumidox® II 96-well LED Array (Analytical Sales and Services, Inc., NJ, USA) equipped 660 nm max LED was used for light irradiation. DNA oligonucleotides were purchased from Integrated DNA Technologies, Inc. (Coralville, IA, USA). Telo24 G4 DNA with the sequence of 5'- TTAGGGTTAGGGTTAGGGTTAGGG -3' was subjected to the pre-annealing process by heating at 90 °C for 10 min and cooling back to room temperature over 3 hours in 10 mM HEPES buffer (pH 7.4, containing 100 mM KCl and 1 mM Na_2EDTA). All measurements were conducted in the same buffer conditions.

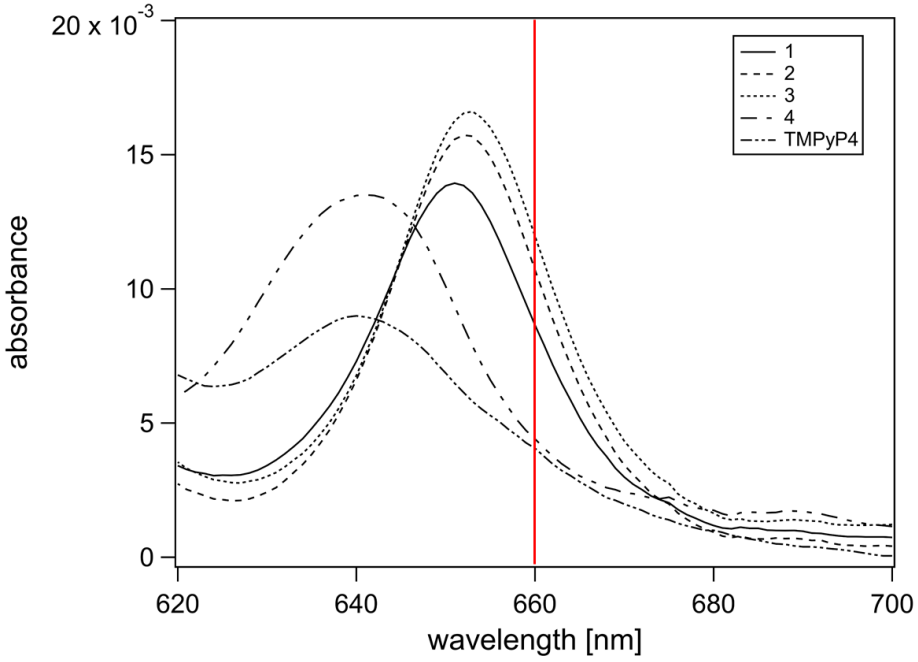

Fig. S43. UV-vis spectra of 5 μM solutions of **1**, **2**, **3**, **4** and TMPyP4 in 10 mM HEPES at 660 nm.

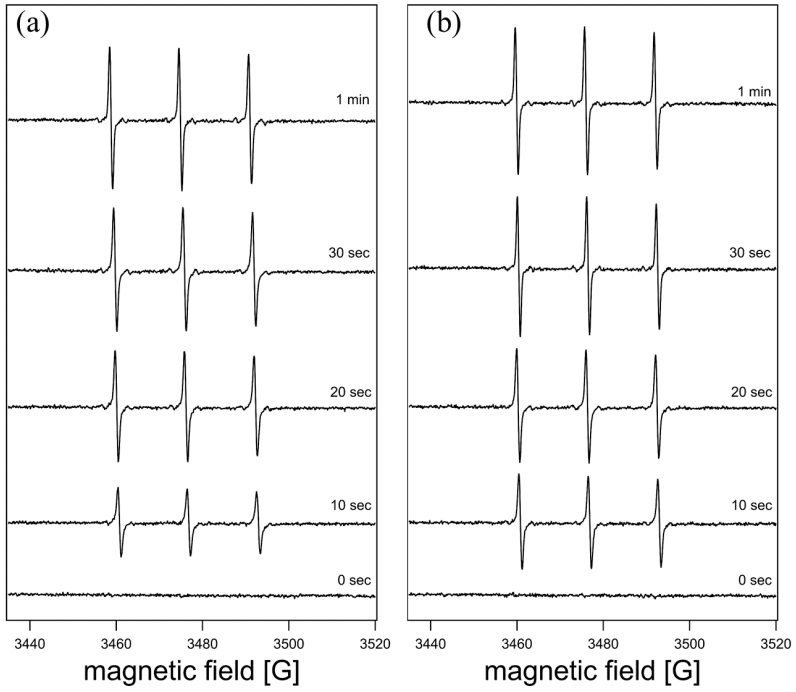

Fig. S44. X-band ESR spectra of 4-oxo-TEMP adduct with $^1O_2$ generated in solution of **1** (a) (50 μM) and **2** (b) in pH 7.4 10 mM HEPES under irradiation by a deep red LED (λmax = 660 nm) for 0, 10, 20, 30 and 60 sec. Experimental conditions: 4-oxo-TEMP 80 mM, temperature 296 K, microwave frequency 9.785 GHz, microwave power 1 mW, modulation amplitude 1.00 G, modulation frequency 100 kHz, scan time 83.89 s.

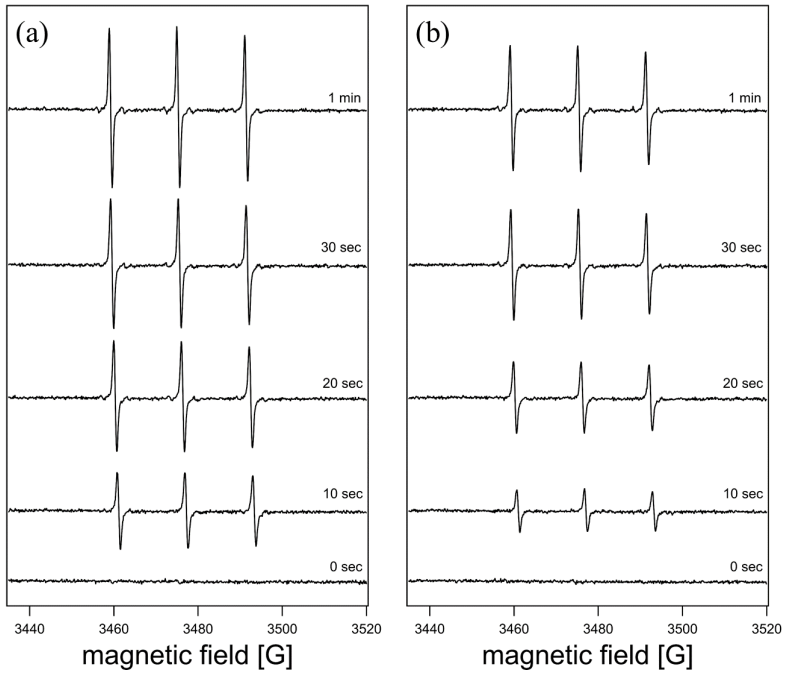

Fig. S45. X-band ESR spectra of 4-oxo-TEMP adduct with $^1O_2$ generated in solution of **3** (a) (50 μM) and **4** (b) in pH 7.4 10 mM HEPES under irradiation by a deep red LED (λ_{max} = 660 nm) for 0, 10, 20, 30, and 60 sec. Experimental conditions: 4-oxo-TEMP 80 mM, temperature 296 K, microwave frequency 9.785 GHz, microwave power 1 mW, modulation amplitude 1.00 G, modulation frequency 100 kHz, scan time 83.89 s.

Amounts of $^1O_2$ generated by the porphyrins were estimated by the double integration of the ESR spectra of 4-oxo-TEMPO, a $^1O_2$ adduct of 4-oxo-TEMP. For a calibration, 5-point standard curve was prepared from the double integration values of ESR spectra of the 4-oxo-TEMPO solutions (0.25 to 4 μM).

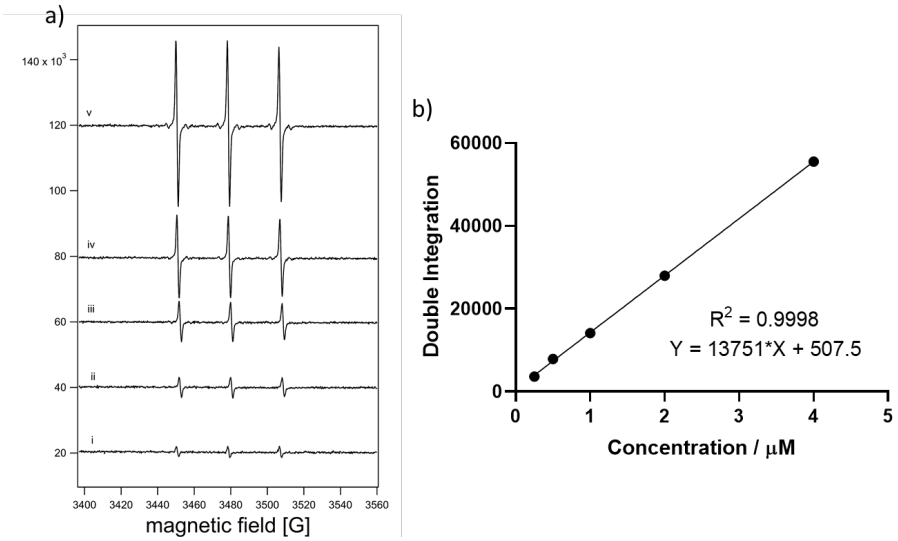

Fig. S46. (a) X-band ESR spectra of 4-oxo-TEMPO at 0.25 μM (i), 0.5 μM (ii), 1 μM (iii), 2 μM (iv) and 4 μM (v) in pH 7.4 10 mM HEPES buffer. Experimental conditions: temperature 296 K, microwave frequency 9.785 GHz, microwave power 1 mW, modulation amplitude 1.00 G, modulation frequency 100 kHz, scan time 83.89 s. (b) Calibration curve of 4-oxo-TEMPO concentration *versus* double integration of ESR spectra.

5. DNA Photocleavage

The pBR322 DNA and Gel Loading Dye, Purple (6X) were purchased from New England Biolabs (Ipswich, MA, USA). Nunc MicroWell 96 Well Round (U) Bottom Plate was bought from Thermo Scientific (Waltham, MA, USA). Ethylenediaminetetraacetic acid disodium salt dihydrate (EDTA), GelRed® Nucleic Acid Stain 10000X and agarose were purchased from Sigma-Aldrich (St. Louis, MI, USA). Lumidox® II 96-well LED Array (Analytical Sales and Services, Inc., NJ, USA) equipped with 660 nm max LED was used for light irradiation. Gel Electrophoreses were performed using Mupid-exU gel electrophoresis system (Mupid Co. Ltd., Tokyo, JAPAN). Imaging of the gels was performed using ChemiDoc Imaging System (Bio-Rad Laboratories, Inc., CA, USA).

The pBR322 DNA was diluted to a stock solution of 25 ng•μL–1 in Tris-HCl buffer (10 mM, pH 8.0, containing 1 mM EDTA). An aliquot of DNA solution (10 μL) was mixed with 10 μL solution of **1**, **2**, **3** or **4** in Milli-Q water. The mixtures were irradiated by 96-well illuminator for 10 min by the light source of 660 nm deep red LED (330 mW/cm^2). Subsequently, Gel Loading Dye Purple 6X (4 μL) was added to each sample to be loaded to an agarose (1% agarose in 0.5X TBE buffer). Electrophoreses were conducted at 100 V for 80 min using 0.5X TBE as the running buffer. The gel was then stained using GelRed® Nucleic Acid Stain 3X (diluted from 10000X by milliQ water) for 1 h. The gels were then imaged using GelRed filter settings to provide the images. The images were analyzed using ImageJ software.

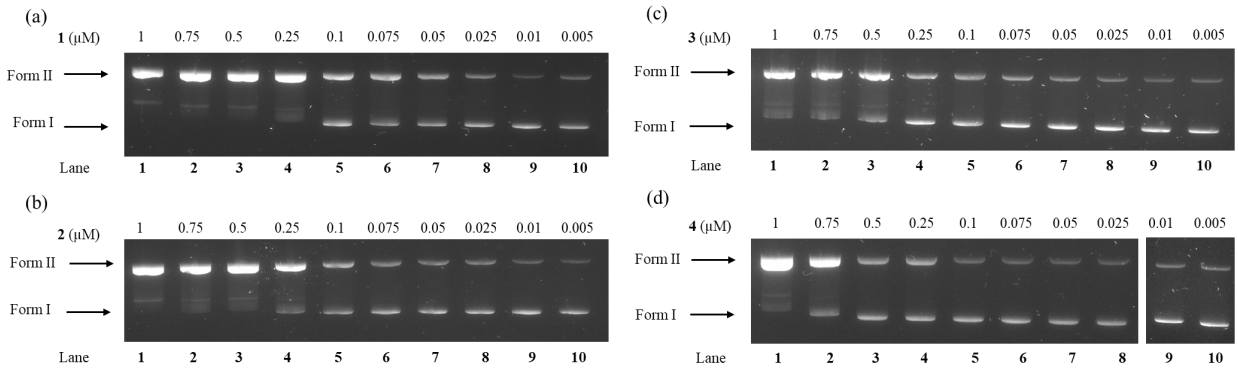

Fig. S47. Photoinduced DNA cleavage of pBR322 DNA by **1** (a), **2** (b), **3** (c) and **4** (d) under irradiation by deep red LED light (λ_{max} = 660 nm) for 10 min. [DNA] = 12.5 μg•mL^{-1} in Tris-HCl-EDTA buffer (pH 8.0).

6. Flow cytometry

Flow cytometry measurements were performed on Cytek® Aurora system (Cytek Biosciences, Fermont, CA, USA). Data were analyzed using FlowJo software with the V12 channel (excitation wavelength: 405 nm; emission wavelength: 692 nm (center) with 28 nm width). Untreated HeLa and NHDF cells were

used for gating by forward (FSC-A) and side scatter (SSC-A) analysis. The population of cell singletons was selected using a forward scatter height (FSC-H) vs forward scatter area (FSC-A) plot.

Table S5. Mean fluorescence intensities of cells analyzed by flow cytometry in Fig. 7.

compounds	Mean Fluorescence Intensity	
	HeLa	NHDF
Control	1730	6580
1	135,000	335,000
2	222,000	496,000
3	330,000	799,000
4	99,500	359,000

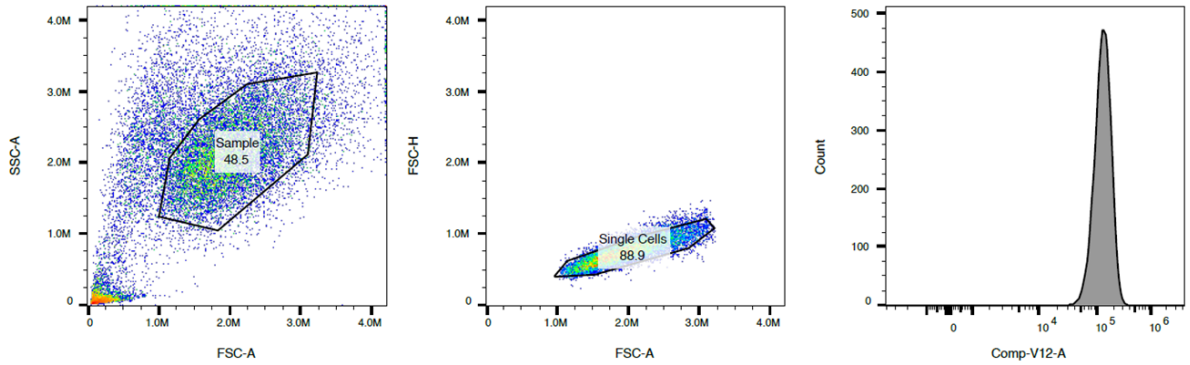

Fig. S48. Gating strategy for the HeLa cells treated with compound **1**.

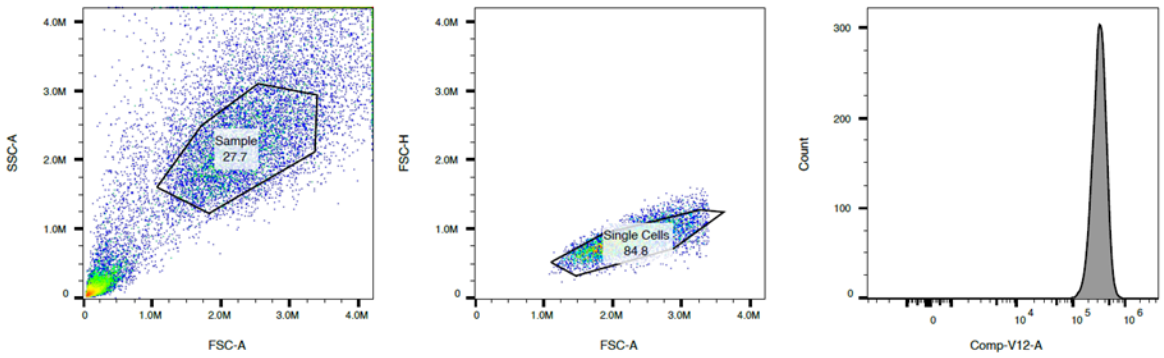

Fig. S49. Gating strategy for the NHDF cells treated with compound **1**.

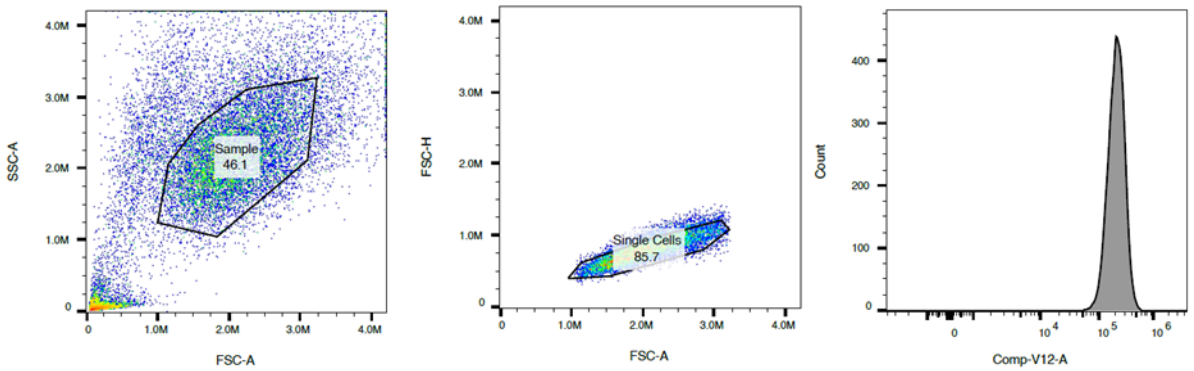

Fig. S50. Gating strategy for the HeLa cells treated with compound **2**.

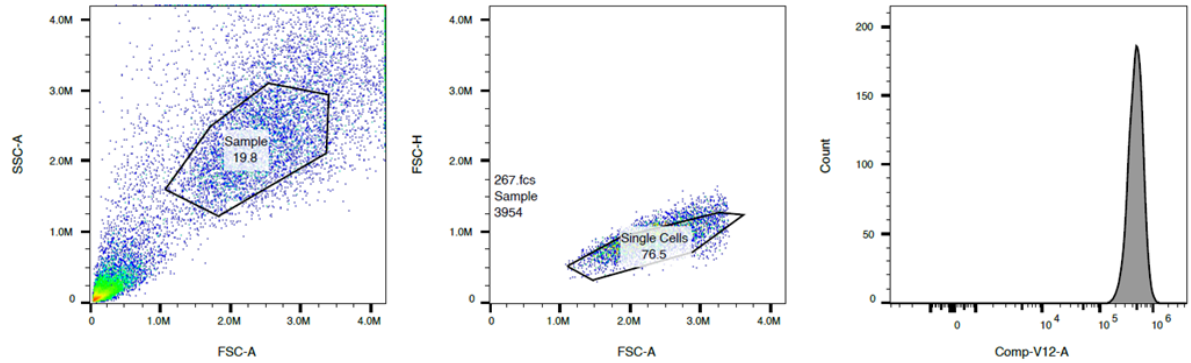

Fig. S51. Gating strategy for the NHDF cells treated with compound **2**.

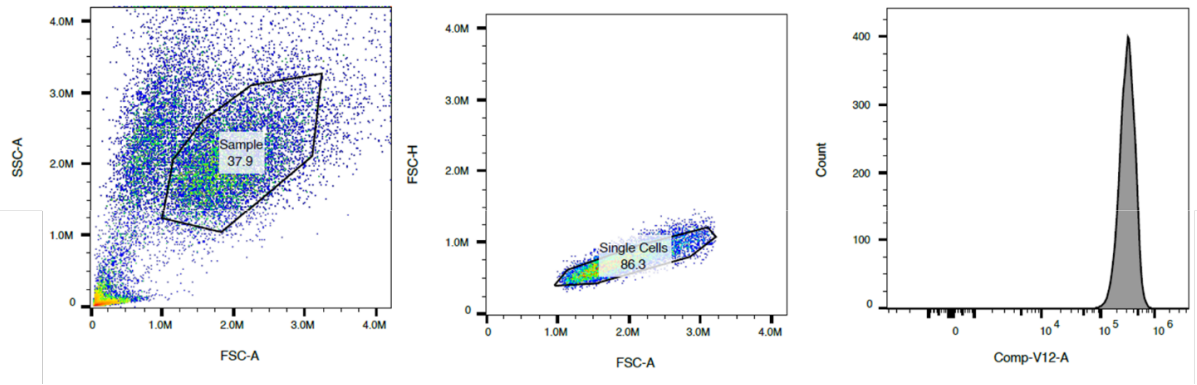

Fig. S52. Gating strategy for the HeLa cells treated with compound **3**.

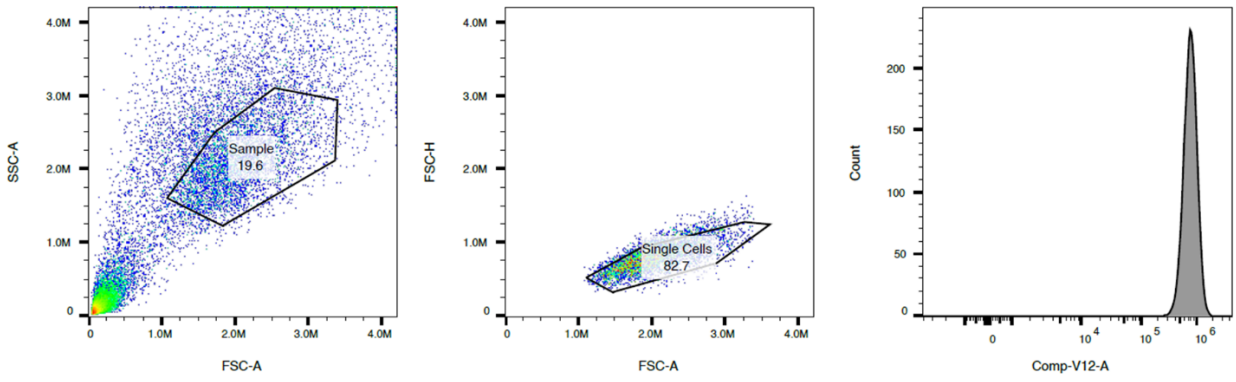

Fig. S53. Gating strategy for the NHDF cells treated with compound **3**.

7. References

1. A. Wolfe, G. H. Shimer and T. Meehan, *Biochemistry*, 1987, **26**, 6392–6396.
2. Ç. Çelik, N. Kakusho, T. Xu, S. Sik Lee, N. Yoshizawa-Sugata, H. Masai and Y. Yamakoshi, *RSC Medicinal Chemistry*, 2026, **17**, 225–235.